11-26-2012

Sinusoidal Endothelial Dysfunction in Non-Alcoholic Fatty Liver Disease.

Sandhya Lakshmi Gopalakrishnan
University of Nebraska-Lincoln, sandhyalakshmi.g@gmail.com

SINUSOIDAL ENDOTHELIAL DYSFUNCTION IN NON-ALCOHOLIC FATTY LIVER DISEASE

By

Sandhya Lakshmi Gopalakrishnan

A THESIS

Presented to the Faculty of

The Graduate College at the University of Nebraska

In Partial Fulfillment of Requirements

For the Degree of Master of Science

Major: Biochemistry

Under the Supervision of Professor Edward N. Harris

Lincoln, Nebraska

November 2012

SINUSOIDAL ENDOTHELIAL DYSFUNCTION IN NON-ALCOHOLIC FATTY LIVER DISEASE

Sandhya Lakshmi Gopalakrishnan, M.S.

University of Nebraska, 2012.

Adviser: Edward N .Harris

Non-alcoholic fatty liver disease (NAFLD) is an asymptomatic increasingly common disorder that affects liver metabolism and is often the precursor for liver pathologies such as fibrosis, cirrhosis and hepato-cellular carcinoma. The liver sinusoidal endothelial cells act as a liver sieve by allowing macromolecules and chylomicrons to traverse through their fenestrations (sieve plates) to hepatocytes. Since liver sinusoidal endothelial cells (LSEC) regulate serum derived macromolecular exposure to hepatocytes, we asked what role LSEC could play in the pathogenesis of NAFLD. To investigate the early events of NAFLD we used a rat model (Sprague-Dawley) in which animals were maintained on standard and high fat diets (HFD) for a period of 8 weeks. The lipid accumulation in the livers, isolated hepatocytes and LSEC were visualized by Oil Red O, BODIPY (boron-dipyrromethene) stains and CARS (Coherent Anti-stokes Raman Scattering) imaging. There was evidence of increased size of lipid droplets in the hepatocytes of HFD rats in contrast to their LSEC, which showed minimal to no lipid accumulation. The lipid content of the liver tissues was analyzed by thin layer chromatography, which revealed the accumulation of triglycerides and cholesteryl esters in the livers of HFD rats compared to the control rats. In vitro endocytosis of ^{125}I-HA (hyaluronic acid) experiments carried out on LSECs isolated from the rat livers showed that the ^{125}I-HA uptake is significantly higher in control rats compared to HFD rats. We also observed that serum HA levels and alkaline phosphatase (ALP) levels were increased in HFD rats, in contrast to alanine transaminase (ALT), triglycerides and cholesterol, which remained the same. Purified RNA from the isolated LSECs was subjected to microarray analysis demonstrating altered gene expression patterns between rats on two different diets. The kidneys, gut, and spleens were also harvested to study the interplay of the organs in the disease. We have been able to demonstrate that decreased endocytic ability of LSECs precedes fibrosis of liver in NAFLD.

DEDICATION

To my mother, for her unwavering belief in me.

ACKNOWLEDGEMENTS

I would like to thank Dr. Edward Harris for his guidance, support and help. I would also like to thank my committee members, Dr. Concetta Dirusso and Dr. Paul Black for their helpful suggestions and consideration.

My family and friends have been a great support to me and I would like to thank them for it. I would also like to thank my husband, Ananth for his constant encouragement and understanding.

TABLE OF CONTENTS

DEDICATION III
ACKNOWLEDGEMENTS IV
TABLE OF CONTENTS V
LIST OF FIGURES VI
LIST OF TABLES VI
CHAPTER 1 1
INTRODUCTION AND LITERATURE REVIEW 1
1.1 Liver 2
1.2 Cells of the liver 2
1.3 Organization of the liver 5
1.4 Structural and functional aspects of sinusoidal endothelial cells 6
1.5 Non-Alcoholic Fatty liver disease (NAFLD) 12
CHAPTER 2 14
ISOLATION OF LIVER SINUSOIDAL ENDOTHELIAL CELLS. 14
2.1 Introduction 15
2.2 Materials and methods 16
2.3 Discussion 20
CHAPTER 3 23
EFFECT OF HIGH FAT DIET ON THE LIVER 23
3.1 Introduction 24
3.2 Materials and methods 25
3.3 Results 28
3.4 Discussion 29
CHAPTER 4 41
SINUSOIDAL ENDOTHELIAL DYSFUNCTION IN FATTY LIVER DISEASE 41
4.1 Introduction 42
4.2 Materials and methods 43
4.3 Results 47
4.4 Discussion 48

CONCLUSIONS AND FUTURE DIRECTIONS..... 58
REFERENCES 66

LIST OF FIGURES

Fig 1: Basic architecture of the liver.....6
Fig 2: Electron micrograph of sinusoidal endothelial cells.....7
Fig 3: Stabilin receptors.....10
Fig 4: Liver cells in fibrosis.....13
Fig 5: Assembly of perfusion apparatus.....18
Fig 6: Culture of isolated liver sinusoidal endothelial cells.....22
Fig 7: Weight of control and high fat rats.....32
Fig 8: Abdominal exposure and visual inspection of livers.....34
Fig 9: Liver tissue staining.....35
Fig 10: Blood chemistry.....36
Fig 11: Liver enzyme measurements.....37
Fig 12: Serum free fatty acid assay.....38
Fig 13: Lipid composition of liver tissue by TLC.....39
Fig 14: Densitometry of TLC data.....40
Fig 15: Staining of isolated hepatocytes and LSEC.....52
Fig 16: SEM micrographs of livers.....53
Fig 17: Serum HA levels.....54
Fig 18: In vitro endocytosis.....55
Fig 19: Western blot of LSEC lysates.....55
Fig 20: qPCR analysis of Stab2 expression.....57

LIST OF TABLES

Table 1: Composition of standard diet.....30
Table 2: Composition of high fat diet.....31
Table 3: Blood Chemistry.....33
Table 4: Summary list of upregulated genes.....56
Table 5: Summary list of downregulated genes.....56

CHAPTER 1

INTRODUCTION AND LITERATURE REVIEW

Chapter 1

Introduction and literature review

1.1 Liver

The liver is the largest visceral organ in humans and other higher vertebrates contributing to about 2-5% of total body weight. It is a principal organ in the body as it maintains the internal homeostasis in the organism. The liver participates in synthesis, storage, export and secretion of various metabolites. Nutrients and other xenobiotics from the intestinal system are transported to the liver where they are metabolized. The liver clears various molecules and cells, foreign antigens and microbes from the blood stream. It has a wide variety of functions and is important for the maintenance of metabolic integrity of the body. The multiple functions of the mammalian liver are a combination of exocrine, endocrine and paracrine functions, carried out by specialized cell types listed below. All these varied functions take place in a unique structurally complex, multicellular tissue, called the liver (1).

1.2 Cells of the liver

The liver consists of seven distinct types of cells - hepatocytes, cholangiocytes, sinusoidal endothelial cells, macrophages, lymphocytes, dendritic cells and stellate cells, arranged in a matrix, which allows them to work in co-ordination to synthesize, metabolize and clear a wide range of molecules. The cells of the liver are supplied with the various molecules by the flow of blood through a uniquely structured capillary system. The sources of blood to the liver are the venous and the arterial blood, which flow through the afferent and efferent blood vessels that interdigitate uniformly. This

vasculature is unique because it is separated by a parenchymal mass of cells and at the same time connected by small capillaries known as the sinusoids (1).

1.2.1 Hepatocytes

The hepatocytes are referred to as parenchymal cells and all the other cells types are broadly termed non-parenchymal cells. The hepatocytes are large polyclonal cells, numerous in number, constitute about 60% of the cells and 80% of the volume of the liver. They are responsible for most of the metabolic and synthetic functions of the liver. The hepatocytes are complex rhomboid shaped and have distinct surfaces for the different functions they carry out. The area of the hepatocyte surface that faces the sinusoid is greatly amplified and shaped into folds known as microvilli, which extend into the space of Disse. Adjacent hepatocytes are held together to form long cords of cells by intercellular adhesion complexes. The intercellular membrane has gap junctions for transport of small molecules between adjacent cells. The intercellular membrane is mostly flat, except at regions where it forms bile canaliculi. The bile canalicular membrane is modified for the secretion of bile. The membrane facing the sinusoidal lumen performs extraction of a wide variety of molecules from the blood and simultaneous secretion of molecules synthesized by the hepatocytes (2). The non-parenchymal cells include stellate cells (HSC), Kupffer cells (KC) and liver sinusoidal endothelial cells (LSEC).

1.2.2 Macrophages or Kupffer cells (KC)

These cells occupy about 2% of the liver. They are located within the sinusoidal lumen, held closer to the LSEC by loose attachments. The KC express C3 and Fc

receptors which clear large particulate material such as bacteria, worn out cells, dead hepatocytes by phagocytosis. The KCs also clear immune complexes, tumor cells, liposomes, lipid microspheres, iron and various other particulate matter. Clearance of circulating endotoxin is one of the most important functions of KCs. Endotoxins activate KCs and result in the secretion of interleukin-1/1α and tumor necrosis factor, reactive oxygen species, and transforming growth factor-β (3-5).

1.2.3 Stellate cells (HSC)

The stellate cells (HSC) are located in the space of Disse between the hepatocytes and the sinusoids and comprise 1.5% of the liver. Stellate cells store retinoids, triglycerides, cholesterol and free fatty acids. HSC also secrete and degrade components of the peri-sinusoidal matrix. During liver injury, these cells respond to inflammatory cytokines such as IL-6 and TGF-β, become activated and acquire a myofibroblastic stage. They undergo morphological changes, start proliferating and become contractile, lose their lipid stores and secrete fibrogenic and inflammatory cytokines, which if left unchecked, lead to fibrosis (6).

1.2.4 Sinusoidal endothelial cells (LSEC)

The liver sinusoidal endothelial cells (LSECs) comprise about 3% of the liver. These cells are flattened and comprised of holes or fenestrations that are grouped together to form sieve plates. The sinusoidal endothelium lacks a basement membrane, which makes it unique from all other endothelial cells. LSECs are responsible for the clearance of various molecules in the blood that flows through the sinusoids. They are also essential components of the liver centered innate immune system, which also includes Kupffer

cells, lymphocytes and dendritic cells (1). Since LSEC are the main focus of our study, the functional aspects of this cell type are discussed in detail in the subsequent sections.

1.2.5 Cholangiocytes

The cholangiocytes are cells that line the bile ducts and form 1% of the liver parenchyma. These cells are responsible for the modification of the canalicular bile composition, which occurs through a series of secretory and absorptive processes (7, 8). Cholangiocytes also interact with other liver cells such as hepatocytes, LSEC, HSC and KC by releasing growth factors, peptides, nucleotides, pro-inflammatory and chemotactic cytokines and other signaling molecules (7). These cells are involved in regulation of bile formation, liver inflammatory processes, angiogenesis and fibrogenesis because of their interaction with the other liver cells (8).

1.3 Organization of the liver

Hepatocytes are arranged in the form of cords through tight junctions that keep them together. Vascular sinusoids are present on either side of the hepatocytes. The space between the sinusoidal endothelium and hepatocytes is known as space of Disse. Stellate cells are present in the space of Disse. The KCs are present in the sinusoidal lumen and are loosely attached to the endothelial cells. The sinusoidal endothelium, because of its position, is in interaction with all other cells of the liver and plays a crucial role in the supply of required material to the hepatocytes and also in the scavenger and immune systems of the liver (Fig. 1). Hepatocytes and other cells communicate by extending their pseudopodia and microvilli through the fenestrations of the LSECs (Fig 2). Fenestrations

permit the passive transport of solutes and regulate the traffic between blood and the underlying hepatocytes (9).

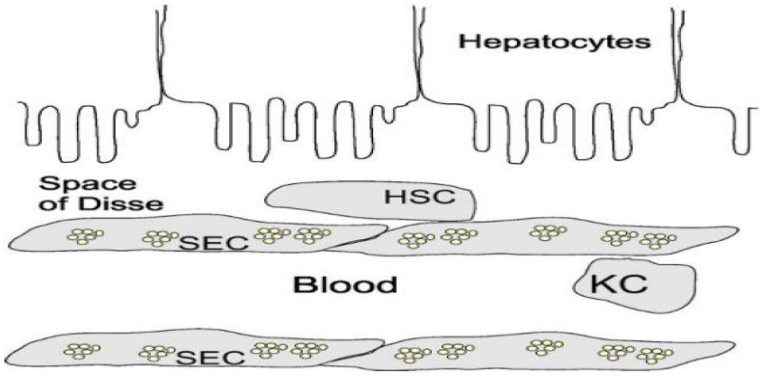

Figure 1: Basic architecture of the liver. LSEC form the walls of the sinusoids and are fenestrated. Stellate cells are found in the space of disse, whereas the Kuppfer cells are found in the sinusoidal lumen. The lumen is lined on both sides by hepatocytes.

1.4 Structural and functional aspects of sinusoidal endothelial cells

Sinusoidal endothelial cells constitute the second most abundant cell type in the liver. They are present between the hepatocytes and blood. The presence of sinusoidal endothelial cells as a unique cell type was not discovered until the perfusion fixation and electron microscopy studies by Wisse et al (10). Although LSEC populations contribute to only 6.3% of the total liver volume, they represent approximately 40% of the total number of hepatic cells (11).

1.4.1 Sieve function of the LSEC

LSEC have a unique morphological phenotype called the fenestrated endothelium. The fenestrated endothelium is a subset of discontinuous endothelium, where the cells have pores traversing the cytoplasm. Each pore is approximately 100 to 150 nm in diameter. Macromolecules larger than 100nm-120nm in diameter or rigid molecules are not allowed to diffuse through the fenestrae, attributing a sieve function to LSEC (12). In

addition to the fenestrated endothelium, the cells also lack an organized basement membrane. The paracrine secretions of the adjacent cells maintain the unique structure of the endothelium. Hepatocytes and HSC secrete vascular endothelial growth factor (VEGF), which stimulates LSEC to constitutively produce nitric oxide (NO) by endogenous nitric oxide synthase (eNOS) (13). The LSEC maintains fenestrations for a longer duration when exogenous VEGF is provided to the cell culture and VEGF induces endothelial fenestrations *in vitro* (14).

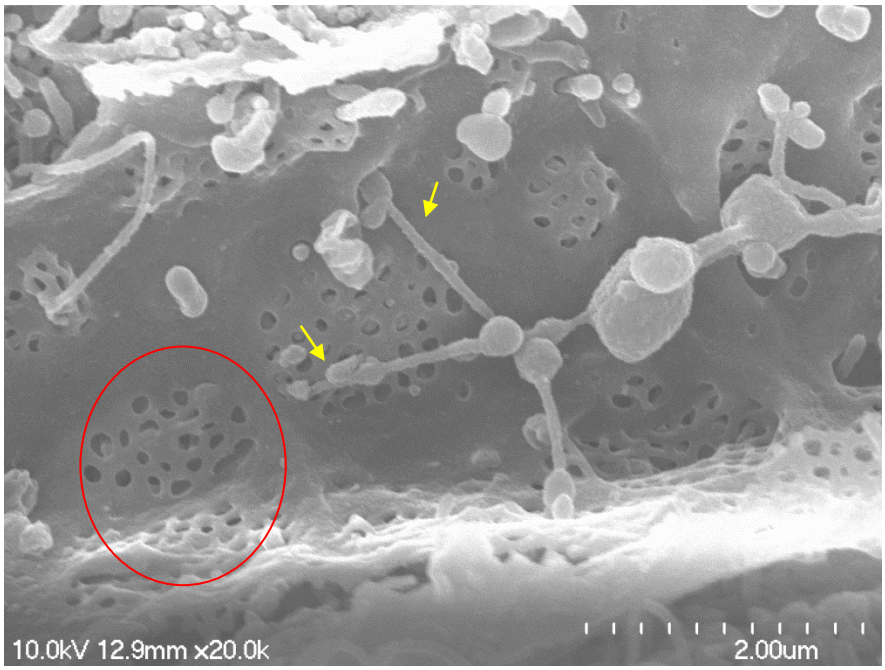

Fig 2: Electron micrograph of sinusoidal endothelial cells, displaying the presence of fenestrae clustered into sieve plates. The encircled region indicates a sieve plate and the arrows point towards microvilli extending through the fenestrations.

LSECs lose their fenestrations in a process called capillarization or de-fenestration due to the formation and deposition of extracellular matrix and build up in the space of Disse resulting in LSEC dysfunction. Deposition of collagen and laminin, and thickening of the LSEC, characterizes defenestration (14). Defenestration precedes

fibrosis and has been observed in various disease conditions such as primary biliary cirrhosis (15), hepatitis (16), specific viral infection of the LSEC (17) and with the venous administration of endotoxin (12, 18).

1.4.2 Functions of sinusoidal morphology

The LSEC fenestration allows chylomicrons and VLDL remnants to pass through the sieve and allows access to the hepatocytes. Blood flow to the liver is a combination of both arterial and venous blood. Normal arterial pO2 is 90-100 mm Hg and the pO2 for portal vein is 45-55 mm Hg. As a result, tissue oxygenation of the liver is lower than that for the other tissues (1). The presence of fenestrae optimizes the delivery of oxygen to the hepatocyte. There are various studies that explore the role of fenestrae in various conditions, such as liposomal transport (19), hydrodynamics (20), liver regeneration (21), the role of VEGF regarding porosity (22), nitric oxide synthesis (23) and old age (24). The fenestrae are important for the process of drug clearance. It allows the passage of bound and unbound drugs to the space of Disse for uptake and clearance by the hepatocytes (12).

1.4.3 Scavenger functions

The LSEC are the primary scavenger system of the liver. They contain numerous coated pits on their surface which creates a cationic surface charge that allows for endocytosis of negatively charged molecules. Different types of scavenger receptors such as hyaluronan receptors, mannose macrophage receptors and Fc gamma receptors are expressed by LSECs, which allow the removal of various macromolecules from the blood such as proteins, polysaccharides, lipids and nucleic acids (25). The LSECs internalize macromolecular waste such as extracellular matrix breakdown products (26), lysosomal

enzymes (27), immune complexes (28), advanced glycation end products (29), acetylated and oxidized low density lipoproteins (30)and modified proteins (31). There are recent studies that suggest that LSECs might be involved in viral clearance

1.4.4 Stabilin receptors

This class of Type I multi-domain transmembrane receptors consists of two proteins, Stabilin-1 and Stabilin-2. Stabilin-1 is expressed by LSECs in liver, spleen, lymph nodes and alternatively activated macrophages (32).They both consist of multiple EGF-like and fasciclin domains and a single X-link domain with amino acid sequences that are 55% identical and 42% similar (Fig 3). The X-Link domain in Stabilin-1 is non-functional in that it does not bind hyaluronan. Stabilin-1 and Stabilin-2 have both common and different ligand binding profiles. Stabilin-1 mediates endocytosis of acetylated LDL (33), SPARC (Secreted protein acidic and rich in cysteine) (34), Advanced glycation end products (AGE)(29), placental lactogen (35) and phosphatidylserine (36, 37). Stabilin-1 functions as a bacteria-binding protein and modulates angiogenesis (38). It helps in the lymphocyte migration and entry of leukocytes to the site of inflammation (39).

Hyaluronic acid (HA) is a matrix polysaccharide with repeated disaccharide units of D-glucuronic acid and N-acetyl glucosamine. HA is a major constituent of the ECM, and serum HA is known to be associated with inflammation, wound healing, and regenerative morphogenesis. Elimination of denatured or excess HA from the circulation is necessary to maintain the normal range of blood viscosity (40). Stabilin-2 is responsible for the efficient uptake of hyaluronic acid and degradation and functions to regulate the amount of HA present in the body (26). In addition, Stabilin-2 receptors

eliminate oxidized LDL and acetylated LDL (41), advanced glycation end products (29), N terminal propeptides of types I and III procollagen (PINP and PIIINP) (31, 36), phosphatidylserine(42) , chondroitin sulfates(43), and high and low molecular weight heparins(44, 45) and small heparin oligos(46). In both rat and human, two isoforms of HARE are present with molecular masses of 175 and 300 kDA or 190 and 315 kDa, respectively. The isoforms are derived from the same precursor, which is the Stabilin-2 protein. Stabilin-2 is a large protein consisting of 2551 amino acids. The full length 315/300 kDa isoform is a type I membrane protein that contains a 2458 extracellular domain which contains four cysteine rich/fasciclin like domains and a LINK domain which binds to hyaluronic acid. The 190 kDa is similar to the C-terminal 1417 amino acids of the 315 kDa and is derived by proteolytic cleavage by unknown mechanisms (47). The clearance of HA by Stabilin-2 receptor has been used as a marker to determine overall health of the liver (48, 49).

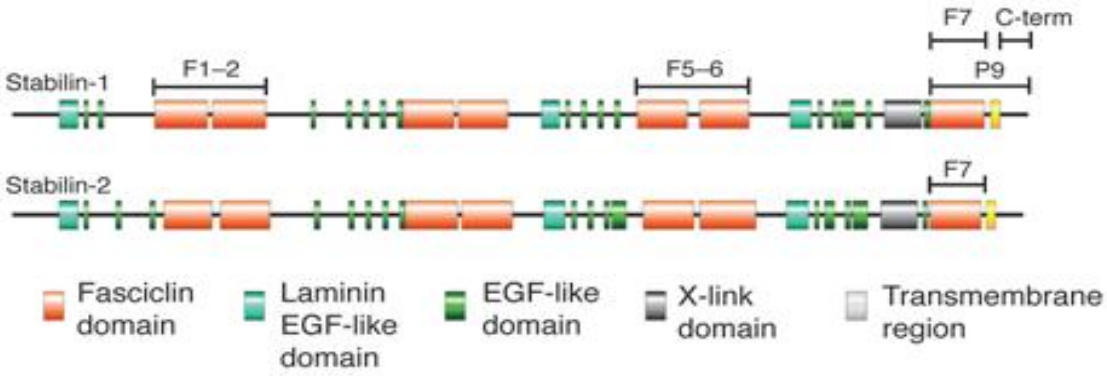

Fig 3: Stabilin receptors of the sinusoidal endothelial cells (36).

The mannose receptor is identical to the macrophage mannose receptor of the Kupffer cells. It is responsible for the removal of waste collagen molecules and

breakdown products that are degraded in the body by collagenolysis. This receptor prevents the accumulation of gelatin, preventing conditions such as intravascular clotting. These receptors facilitate calcium dependent clearance of glycoconjugates, which have mannose residues at their terminus. The mannose receptor is involved in the uptake of the lysosomal enzymes, tissue plasminogen activator and the carboxy-terminal properties of type I procollagen (50). The Fc gamma receptor of the LSEC is similar to the receptors on Kupffer cells. These receptors are involved in the receptor-mediated endocytosis of immune complexes (51, 52).

1.4.5 Secretory functions

The release of prostanoids from KC and LSEC following exposure to endotoxin triggers glycogenolysis in hepatocytes (53). The release of nitric oxide (NO) from LSEC potentiates calcium signaling in surrounding hepatocytes (23). LSEC synthesize and secrete fibronectin (54) and secretes endothelin, a potent vasoconstrictor, on exposure to endotoxin treated Kupffer cells (55).

1.4.6 Sinusoidal dysfunction

The sinusoidal endothelial function is affected in various pathological conditions. The fibrosis of liver is preceded by capillarization of the sinusoidal endothelium (56). Capillarization promotes fibrosis as the capillarized LSECs activate the hepatic stellate cells, which play an important role in the development of fibrotic liver (57). The capillarization of LSEC also affects the delivery of oxygen to the hepatocytes and causes hepatocyte hypoxia. The clearance of chylomicron remnants is affected by the size of LSEC fenestrae. The normal function of the fenestrae prevents atherosclerosis due to proper clearance of chylomicrons (58). Loss of endothelial fenestrae in liver cirrhosis

may contribute to loss of hepatic function because of impaired exchange between sinusoidal blood and hepatocytes. In aging animals, a process known as psuedo-capillarization is observed with the thickening of the LSEC, marked reduction in size and number of fenestrae and an incompletely formed basement membrane (59). In response to injury, LSEC increase their production of cellular fibronectin (60).

1.5 Non-Alcoholic Fatty liver disease (NAFLD)

NAFLD is one of the rising health concerns in both the developing and developed countries. It includes a spectrum of diseases ranging from simple infiltration of fat into the liver tissues (steatosis) to cirrhosis and cancer. NAFLD is considered the hepatic manifestation of metabolic syndrome, which includes type 2 diabetes mellitus, hyperlipidemia, obesity and insulin resistance. The pathology of NAFLD is not clear. Obesity and insulin resistance pose a high risk for development of NAFLD (61). NAFLD begins as a simple deposition of fat in the hepatocytes. The accumulation of fat occurs due to various early mechanisms. These include excessive intake of calories composed of a variety of fats and carbohydrates, coupled with obesity (62), and excessive consumption of high fructose foods/drinks, resulting in impaired lipid metabolism (63). There is an increase in the export of fatty acids from adipose tissue and intestine to the liver. As the amount of fatty acids imported by the liver is higher than the amount needed by it, the excess results in an accumulation of triglycerides in the liver. Hyperinsulinemia causes increased fat storage by the liver. Insulin resistance results in increased triglyceride synthesis, fatty acid uptake and peripheral lipolysis resulting in fat accumulation in the liver (64, 65). Uncontrolled steatosis coupled with the other risk factors proceeds to fibrosis of the liver. In fibrotic conditions, the stellate cells are activated and attain a

myofibroblastic stage. They secrete cytokines and extracellular matrix, resulting in the augmentation of fibrosis. The fenestrae of the sinusoidal endothelium are lost and the development of basement membrane occurs, resulting in capillarization of the sinusoidal endothelium. The hepatocytes lose their microvilli and proceed to apoptosis. The Kupffer cells are activated and secrete inflammatory cytokines (Fig 4). Sinusoidal endothelial cells are known to maintain stellate cells in their dormant stage (66). Recent studies show that LSEC dysfunction precedes inflammation and fibrosis in NAFLD (67), suggesting that the LSEC might be responsible in initiating the fibrotic conditions. In NAFLD, capillarization of sinusoidal endothelium has been observed (68) and serum HA levels were found to be elevated (69). There is no known direct correlation between sinusoidal dysfunction and NAFLD, which forms the focus of this study.

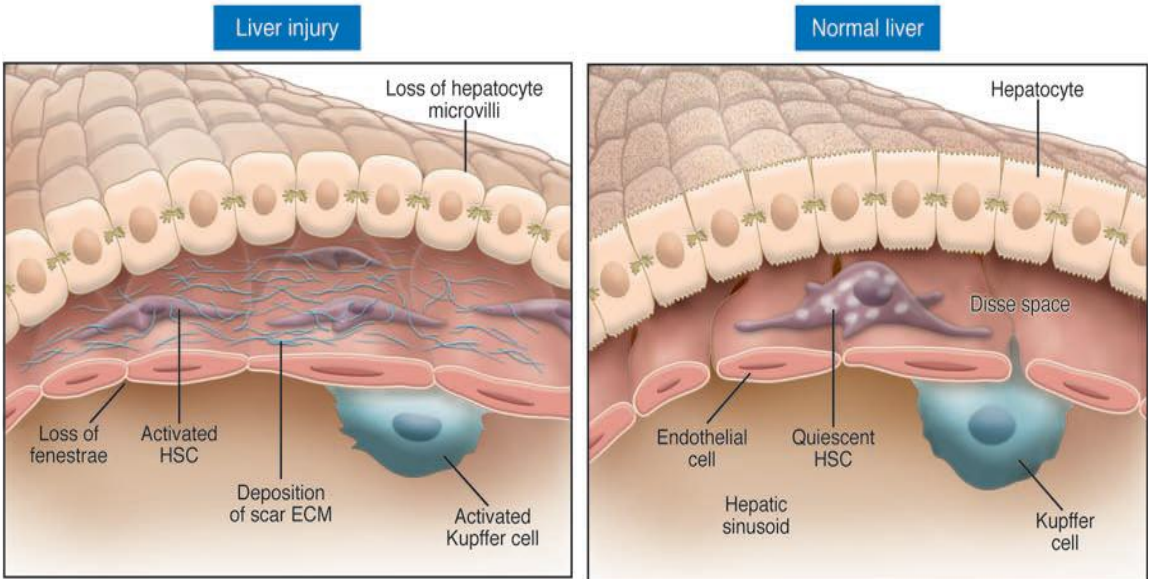

Fig 4: Cells in liver fibrosis and injury (70).

CHAPTER 2

ISOLATION OF LIVER SINUSOIDAL ENDOTHELIAL CELLS.

(Note: This method described in this part has been published)

(Gopalakrishnan Sandhya and Edward N. Harris. "In vivo Liver Endocytosis Followed by Purification of Liver Cells by Liver Perfusion." *Journal of visualized experiments: JoVE* 57 (2011)).

Chapter 2

Isolation of liver sinusoidal endothelial cells

2.1 Introduction

The liver is the metabolic center of the mammalian body and serves as a filter for the blood. The basic architecture of the liver is majorly composed of hepatocytes (~ 80 %) and the remaining of the cellular mass is composed of Kupffer cells (KCs), stellate cells (HSCs), and sinusoidal endothelial cells (LSECs). LSECs form the blood vessel walls within the liver and contain specialized morphology called fenestrae. Fenestration of the cytoplasm is the appearance of holes (~100 μm) within the cells so that the LSECs act as a sieve in which most macromolecules, but not cells pass through to the hepatocytes and HSCs. Due to the lack of a basement membrane, the gap between the LSEC and hepatocytes form the space of Disse (71). HSCs occupy this space and play a prominent role in regulation and response to injury, storage of retinoic acid and immuno-regulation of the liver (72). LSEC are among the most endocytically active cells of the body displaying an array of scavenger receptors on their cell surface. These include SR-A, Stabilin-1 and Stabilin-2. Generally, small colloidal particles less than 230 nm and macromolecules in buffer phase are taken up by LSEC, whereas large particles and cellular debris are endocytosed (phagocytosed) by KCs (73). Thus, the bulk clearance of extracellular material such as the glycosaminoglycans from blood is largely dependent on the health and endocytic functions of LSEC. An increase in blood hyaluronan levels is indicative of liver disease ranging from mild to more severe forms (74).

LSEC de-differentiate under standard culture conditions and must be used within 1 or 2 days upon isolation from the animal. With the exception of one report (75), there

are no immortalized LSEC cell lines in existence. Even this immortalized cell line is de-differentiated in that it does not express scavenger receptors that are present on primary LSEC (our data, not shown). All cell biological studies must be performed on primary cells obtained freshly from the animal. Differentiation of LSEC is marked by the decreased expression of Stabilin-2 or HARE receptor, CD31, and the presence of cytoplasmic fenestration (47). Differentiation of LSEC can be extended by the addition of VEGF (76) in culture media or by culturing cells in hepatocyte conditioned medium (77). The following protocol is adopted from (78, 79) with modifications (45, 80).

2.2 Materials and methods

2.2.1 Excision of liver

10 mL of 30% isoflourane in polyethylene glycol was added to a petri dish in a closed 5.5 L chamber and allowed to equilibrate within the chamber. The rat was anesthetized by placing it in the sealed chamber. Some cotton balls were put in a 30 mL syringe tube and 2 mL of 30% isoflourane was added to it. The anesthetized rat was placed on its back on a diaper-covered tray and the syringe tube was placed over the snout. The entire abdominal cavity was exposed using bandage scissors and forceps. Two strands of surgical silk or polyester thread (ligature) were drawn beneath the vena porta immediately above the mesenteric branch using forceps. The forceps was withdrawn and a loose overhand knot was tied. The vena porta was cannulated with an Insyte autoguard catheter (18 GA, 1.3 x 300 mm, BD Biosciences). The needle was retracted by releasing the spring-loaded trigger on the catheter. The overhand knot was tightened and secured with another knot. The descending aorta (aorta abdominalis) was severed to allow blood

to drain from the circulatory system. The liver was flushed with oxygenated tris buffered saline (TBS, 154 mM NaCl, 10 mM trizma base salt, pH 7.4) at 37°C to remove the blood at a flow rate of 20 mL/min. The liver turned from reddish purple to a loam color. The liver was excised while being flushed by cutting away the GI tract and connective tissue. The liver was placed on a plastic net over a funnel that allows buffers to be collected and re-circulated and flushed for 10 min. The schematic of the perfusion apparatus is illustrated in Fig 5.

2.2.2 Digestion of the liver by collagenase digestion

Freshly dissolved and filtered (0.45 μm) collagenase (100 mg/kg rat weight) was added to 60 mL of Perfusion buffer 2 (67 mM NaCl, 6.7mM KCl, 4.8mM $CaCl_2.H_2O$, 10 mM HEPES,15% BSA, pH 7.4). The pump was stopped and the inlet tubing was exchanged from the TBS flask to the collagenase solution. Immediately after flushing, the digestion with collagenase was begun in a circulatory loop at a flow rate of 20 mL/min, for up to 15 min. After flushing with collagenase, the pump was stopped, the catheter was removed and the liver was transferred to a dish containing 20-30 mL of perfusion buffer 1(142 mM NaCl, 6.7mM KCl, 10mM HEPES, 1.5% BSA, pH 7.4). The Glisson's capsule was peeled from the liver and the cells were shaken out in the liquid. As the liquid becomes opaque with cellular material, the cells were transferred through a 100 μm mesh, followed by filtration through a 30 μm mesh and then into a 50 mL conical tube on ice. More Buffer 1 was added to the liver and cells were shaken from the liver matrix, transferring the liquid to the mesh filters and conical tube. The above steps were repeated until no more cells can be dislodged with reasonable shaking of the liver.

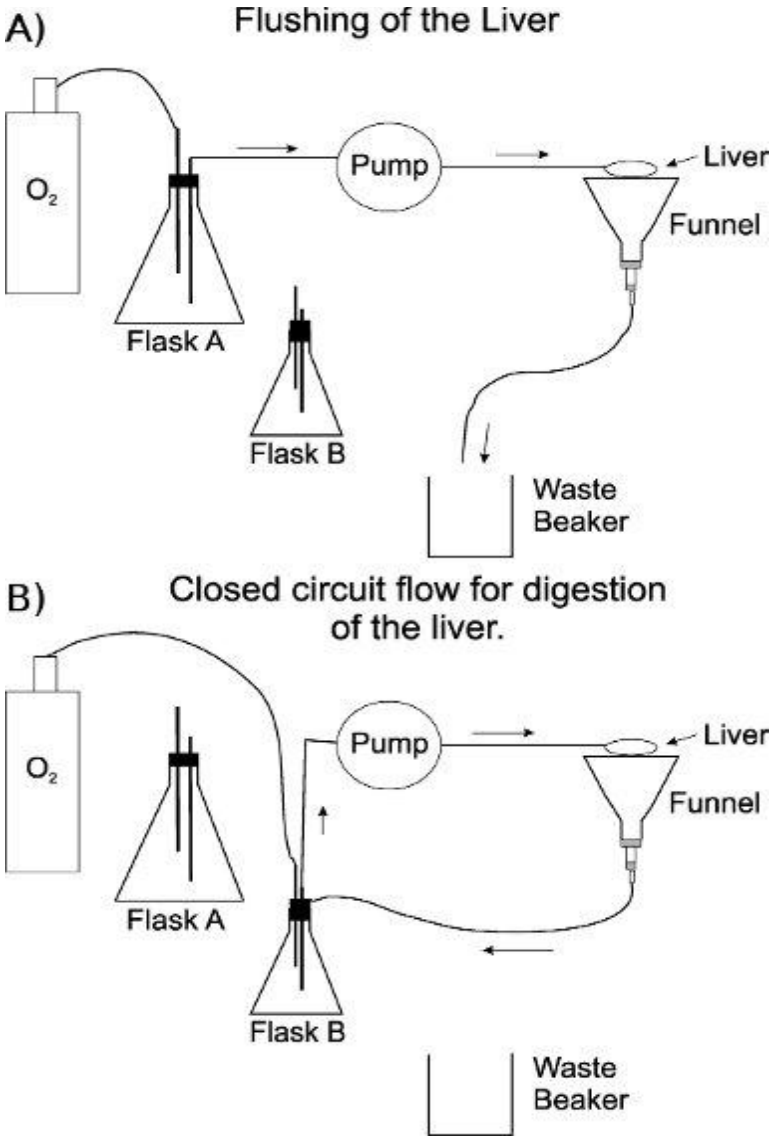

Fig 5: Schematic of the perfusion apparatus. A) Set-up of apparatus during the flushing/washing of the sinusoids of the liver, TBS is in a 1 L flask. B) A 125 mL flask containing ~60 mL Buffer 2 with collagenase is used for digestion of the liver in a closed circuit. The effluent line is also changed from the waste container to flask B through a notch cut in the rubber stopper. The oxygen line is not submerged into the buffer containing collagenase (flask B) to avoid foaming. The stoppers on each flask are notched to allow efficient transfer of the effluent line and to prevent increased pressure from the oxygen gas.

2.2.3 Hepatocyte and LSEC purification

The 50 mL conical tubes containing cells were centrifuged at 150 x g for 3 min to pellet the hepatocytes. The liquid fraction containing non-parenchymal cells was transferred to fresh 50 mL conical tubes on ice. The hepatocytes were washed by re-suspending the pellet in perfusion buffer 3 (137mM NaCl,4.7mM KCl,0.7mM $MgSO_4$,1.2mM $CaCl_2.2H_2O$,10mM HEPES,1.5% BSA, pH 7.4) and the washes were repeated two more times. At the end of the washes, the pellets were ≥97% pure hepatocytes. The LSEC were obtained by centrifuging all of the tubes containing the pooled supernatant (containing HSCs, LSEC, and KCs and some small hepatocytes) at 200x g for 10 min at 4°C. The buffer was aspirated and all the pellets were re-suspended in a total of 35 mL RPMI/BSA (15g/L BSA in RPMI) at 4°C and centrifuged at 100 x g for 3 min. The top 25 mL of liquid was collected and transferred to a clean 50 mL conical tube. The pellet was re-suspended in the remaining 10 mL media and 25 mL of cold RPMI/BSA was added and centrifuged at 100 x g for 3 min. The above steps were repeated, and the cell pellet was discarded along with 10ml media. The supernatants were centrifuged to pellet LSECs, KCs, and HSCs at 200 x g for 10 min at 4°C. Meanwhile, percoll gradients were prepared by adding 20 mL 25% percoll in PBS on ice and then underlaying with 15 mL 50% percoll in each tube.

The cell pellets were re-suspended in a total volume of 30 mL RPMI/BSA. Each gradient was carefully overlaid with 10 mL of cells and centrifuged at 900 x g for 20 min at 4°C. LSECs and KCs have very close buoyant densities and collect at the 25/50% interface. HSCs are typically at the 25%/media interface due to their higher buoyancy as lipid storing cells. Any remaining hepatocytes and blood cells have the lower buoyancies

and are pelleted. The media and stellate cells were aspirated from the top down near the 25/50% interface and the cells in the 25/50% interface were collected and transferred to a fresh conical tube with cold RPMI. The final volume was adjusted to ~40 mL to dilute out the percoll. The conical tube was centrifuged at 350 x g for 10 min at 4°C to pellet the cells. The cells were resuspended in ~10 mL pre-warmed RPMI at 37^0 C containing 100 U/mL penicillin, 100 µg/mL streptomycin and the cells were placed in an acid-washed glass-crystallizing dish. The cells were incubated for 15 min at 37°C in a tissue culture incubator. The LSECs in the supernatant were collected from the dish by rocking. The KCs adhere to the glass much more rapidly than LSECs. Alternatively, LSECs may be separated from KCs by immunopurification using anti-CD31 or anti-Stabilin2/HARE antibodies conjugated to magnetic beads. Viability and cell numbers were assessed by trypan blue exclusion using a hemacytometer or with using an automated cell counter. The LSECs were cultured on fibronectin-coated plastic dishes (Fig 6) at 37°C, 5% CO_2, RPMI/0.25% BSA with 40 ng/mL VEGF, 100 U/mL penicillin, 100 µg /mL streptomycin or with hepatocyte conditioned media. The LSECs was assessed for internalization of I^{125}-HA.

2.3 Discussion

Anesthesia of the rat by the hanging drop method in which isoflourane vapor induces unconsciousness is the preferred method for our studies. A vaporizer may also be used instead of a syringe with cotton to maintain the animal outside the chamber, but the surgical procedures are so quick, it is not required. Polyethylene glycol is added to the isoflurane to decrease the vapor pressure and evaporation rate. Too much isoflurane

vapor will induce death too quickly. If the animal dies before the liver is cannulated and blanched with TBS, pooling blood may clot in the liver and prevent efficient washing of the sinusoids and digestion with collagenase. Gey's buffered saline solution (GBSS) is often substituted by other laboratories for the purification of LSECs. While it is useful for LSEC purification, hepatocytes do not tolerate GBSS as well as Buffers 1-3 and viabilities are not nearly as high. When measuring endocytosis, it is good practice to measure background levels in the organ and in purified hepatocytes. This method is one of two for efficient purification of LSECs following the liver perfusion with collagenase.

The other method separates the non-parenchymal cells by elutriation centrifugation (81), instead of percoll gradient. The advantages for using elutriation over percoll gradients are slightly higher cell viabilities and numbers. The downside is that elutriation centrifugation requires a specialized rotor, dedicated centrifuge, and peristaltic pump together which costs tens of thousands of dollars. This method only requires the use of a refrigerated table-top centrifuge and peristaltic pump which is standard in many laboratories. Separation of LSECs and KCs by selective adhesion is a standard method (82, 83). While it is true that SECs will adhere to the glass and plastic, the key point is to use acid-washed clean glass with no more than 15-minute incubation at 37°C at 5% CO_2. KCs will always adhere faster than LSECs and it is advisable to gently wash the KCs with media to extract any remaining LSECs that have become loosely attached. Pronase and other proteases are also omitted from the collagenase digestion steps in this protocol to increase viabilities of the cells. Proteases digest extracellular receptors and may inhibit cellular adhesion in the final purification steps. The method presented here has a wide variety of applications. Perfusion of the liver for obtaining primary hepatocytes, KC,

LSECs, and HSCs may be useful for a number of studies involving metabolic pathways, immunoregulation, scavenger activities, and other physiological studies. The most difficult part of this procedure is good cannulation, digestion of the liver, and handling of the liver without having the catheter slip from the portal vein.

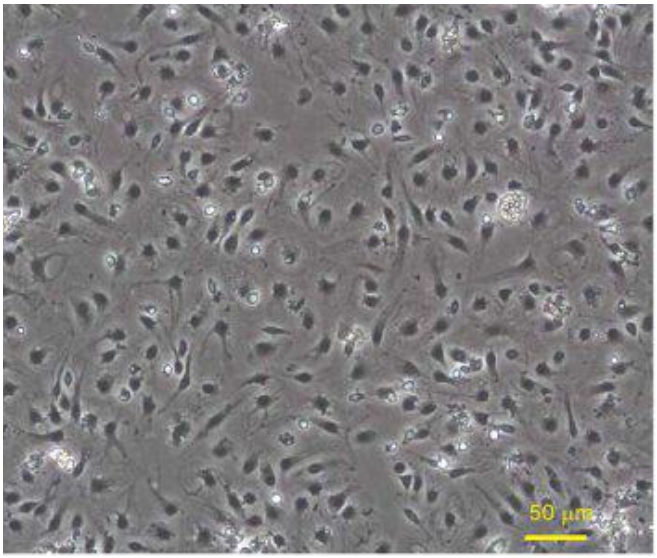

Fig 6: LSECs plated on fibronectin coated plastic 6-well dishes were incubated overnight in RPMI supplemented with 0.1% BSA. Phase contrast images were taken at 100x magnification.

CHAPTER 3

EFFECT OF HIGH FAT DIET ON THE LIVER

Chapter 3

Effect of high fat diet on the liver

3.1 Introduction

The liver is central to the maintenance of energy balance as it regulates the supply of glucose, ketone bodies, lipoprotein and triglycerides to peripheral tissues. Thus, it acts as the primary processing center for the dietary derived lipids and glucose. The liver stores excess glucose as glycogen and excess dietary-fatty acids and excess adipose tissue-derived fatty acids in the form of triglycerides. In conditions of fasting or energy insufficiency, the liver increases synthesis of very low-density lipoproteins (VLDL), β-oxidation of fatty acids and ketogenesis. As the liver plays an important role in proper metabolic handling of fatty acids, impairment of fatty acid storage in the liver due to increased lipid intake poses as an important factor for the development of the metabolic syndrome which includes insulin resistance, Type 2 diabetes, non-alcoholic fatty liver disease (NAFLD), and cardiovascular disorders (84).

It has been observed that serum triglycerides, liver enzymes serum alanine transaminase and alkaline phosphatase, cholesterol, serum HA are increased in NAFLD (85). Fibrosis begins to develop in the liver due to high fat diet ingestion and NAFLD (86). The following experiments were performed to evaluate the condition of the liver and observe if fat accumulation has occurred and if fibrosis has initiated, in the livers of the rats fed on high fat diet. Whole tissues were stained with H&E, Oil Red O and subject to Coherent Anti-stokes Raman Scattering (CARS) microscopy. H& E is a combination of two dyes, haematoxylin and eosin. Haematoxylin stains the acidic parts of the cell like

the nucleus and nuclear material, whereas, eosin stains the basic components of the cell such as proteins. This staining technique helps to visualize the morphology of the tissues. Oil Red O is used to detect neutral lipids in the tissues. The staining is based on the capability of the lipids to dissolve in the dye (87). CARS is a technique used to visualize the lipids in tissues or individual cells. It is a label free imaging technique which is highly sensitive and capable of visualizing lipid rich structures. CARS microscopy relies on the intrinsic molecular vibration for contrast mechanism. It is particularly sensitive to the lipid-rich structures due to the abundance of the CH_2 group and the distinctive CH_2 stretch-vibration frequency at 2840 cm^{-1} (88).

3.2 Materials and methods

3.2.1Sample collection

Four week old Sprague-Dawley rats were maintained on standard diet (12% energy from fat) or high fat diet (60% energy from fat) for 8 weeks. The diet was manufactured by Testdiet and the composition of the diets is given in table 1. The weight of the rats was measured every week. On the completion of the 8th week, the rats were sacrificed and tissues harvested. The rats were fasted for 2 hours prior to sacrifice. The cells of the liver were separated by the perfusion technique described in chapter 2. Blood was collected from the aorta abdominalis during the surgical procedure. Plasma was collected from blood and was stored at -80^0 C for later analyses. Liver, kidney, spleen, fat pads tissues were stored at -20^0 C after adding RNAlater RNA stabilization reagent (Qiagen) for future use.

3.2.2 Biotinylation of advanced glycation end products (AGE)

Advanced glycated end-products (AGE) are the lipids or proteins that have been glycated due to prolonged exposure to sugars (89). The AGE products in the serum are biotinylated to prevent the reduction of these molecules and enable storage for longer duration. 300 µL of plasma was immediately mixed with 300 µL of 10 mM biotin hydrazide to a final concentration of 5 mM biotin hydrazide and the mixture was allowed to react for 2 h at room temperature. After addition to the sample of an equal volume of 30 mM sodium cyanoborohydride in PBS, the mixture was stored in an ice bath for 45 min for promoting the reduction of the Schiff base formed in the hydrazide reaction. The mixture was subjected to dialysis against PBS, to remove excess reagents (90). The advanced glycation end products were collected for mass spectrometric analysis.

3.2.3 Histology of the liver

The liver tissues were fixed in 10% PBS-buffered formalin and subject to two staining procedures: H&E staining and Oil Red O performed at the Veterinary Diagnostic Center, UNL.

3.2.4 Blood chemistry

The liver profile was measured using Vetscan chemistry analyzer (Abaxis). The VetScan Mammalian Liver Profile reagent rotor used with the VetScan Chemistry Analyzer utilizes dry and liquid reagents to provide veterinary *in vitro* quantitative determinations of alanine aminotransferase (ALT), albumin (ALB), alkaline phosphatase (ALP), bile acids (BA), total bilirubin (TBIL), total cholesterol (CHOL), gamma glutamyl transferase (GGT), and (blood) urea nitrogen (BUN) in heparinized whole

blood, heparinized plasma, or serum (Abaxis vetscan protocol). Heparinized whole blood was used for the analysis. Triglyceride levels in the serum were measured using a triglyceride assay kit (Cayman Chemical) according to the manufacturer's instructions. Free fatty acids were measured using Bioassay systems Enzychrom free fatty acid assay kit.

3.2.5 Thin layer chromatography of lipids

Liver tissues of control and HFD rats were frozen at -80^0 C immediately after excision. They were thawed on ice on the day of the experiment for use. Fifty mg of liver tissue was weighed and used for lipid extraction. The tissue was homogenized in 3 mL of chloroform: methanol (2:1) solution containing 0.05% BHT (butylated hydroxy toluene). The homogenate was transferred to a glass tube and shaken at room temperature for 1 hr. Then it was centrifuged at 2500 rpm for 10 min. The supernatant was collected and 2 mL of 0.9% KCl was added and mixed well by vortexing. It was set aside for ~ 20 min until a phase separation was seen. The upper phase was carefully aspirated. The lower phase was transferred to another tube and centrifuged for 5 min at 2000 rpm. The pellet was obtained and resuspended in chloroform. The sample tubes were sealed under argon gas for longer storage periods to avoid lipid peroxidation. The samples along with triglyceride and cholesteryl ester standards were loaded on K5 20 X 20 TLC plates using a TLC spotter. The solvent system used was Hexane: Ether: Acetic acid (8:2:0.1). The bands were developed by placing the TLC plate in iodine vapor saturated container. The intensity of the bands was measured using densitometry by ImageJ.

3.3 Results

The weight gain of the HFD rats and control rats over the period of 8 weeks and was not significantly different (Fig 7). The visual examination of the livers from the control and HFD rats revealed a distinct morphological difference. The livers of the HFD rats look mottled and yellowish in color compared to the control (Fig 8). The livers of the HFD rats show increased lipid accumulation compared to the livers of the control rats, as evidenced by the H& E staining and Oil Red O staining (Fig 9). Huge lipid droplets were observed in the livers of HFD rats compared to the control rats, by CARS imaging (Fig 9).

Though there are various studies that indicate that there is an increase in serum triglyceride and serum cholesterol in NAFLD (91), our experiments showed that the serum triglyceride, serum cholesterol of the HFD rats were not significantly different from the control rats (Fig 10) suggesting transport systems for fatty acids is not impaired. We observed an increase in serum alkaline phosphatase levels in the HFD rats, whereas the levels of serum ALT were not significantly different (Fig 11). Though a significant difference in serum triglyceride was not observed, thin layer chromatography of the lipids isolated from the livers of the control and HFD rats reveals that there is an accumulation of triglyceride and cholesteryl ester in the livers of the HFD rats (Fig 13). Densitometry measurements show a statistically significant difference in the accumulation of triglycerides and cholesteryl ester in the HFD livers compared to the control (Fig 14). The serum of the HFD rats shows an increased free fatty acid content (Fig 12), though the difference is not statistically significant due to low sampling number (n=4).

3.4 Discussion

The ingestion of high fat food by the rats for a period of 8 weeks has resulted in significant changes in their livers compared with the rats maintained on control diet. The liver shows significant damage and is in the initial stages of fibrosis. They show an increased accumulation of lipid, especially triglycerides and cholesteryl ester. Though there is no significant change in liver enzyme, ALT, serum triglyceride and serum cholesterol values, there is a significant increase in serum ALP, which is indication of liver damage and injury. An increase of serum free fatty acid could be observed in the HFD rats, which indicates the increased lipolysis observed in insulin resistance. All these experiments show that this diet was a successful model for initiating lipid accumulation and resulting in NAFLD in the rats.

Though there are various studies about the increase of serum triglycerides, cholesterol and aminotrasferases in non-alcoholic fatty liver disease (61, 84). The levels of serum alkaline phosphatase alone is elevated in our observations. It is concurrent with observations of another study where only the elevation of serum alkaline phosphatase levels are observed (92). Alkaline phosphatase levels are generally increased in conditions of biliary obstruction (93). The relation between sinusoidal endothelial dysfunction and biliary obstruction is an interesting aspect to investigate.

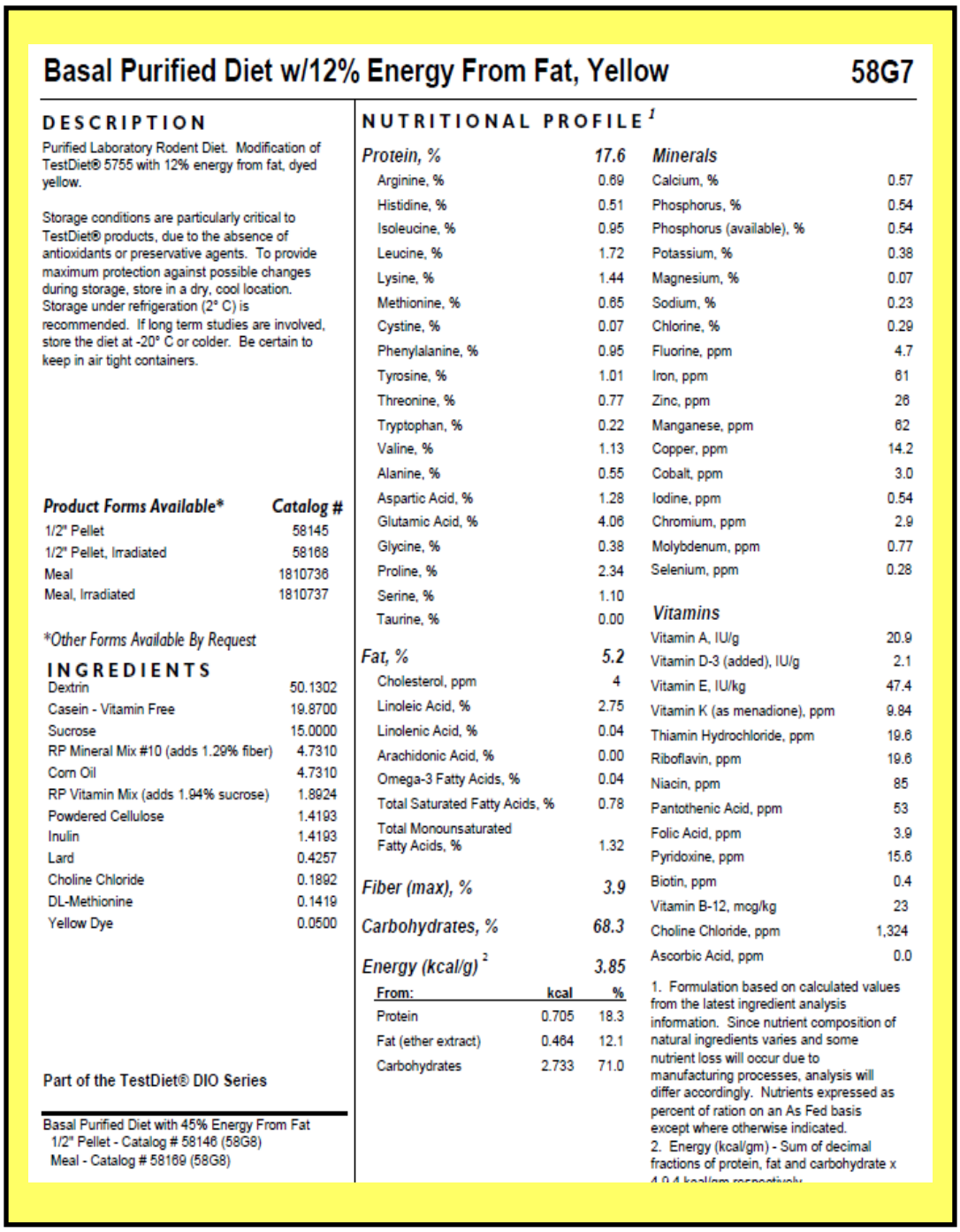

Basal Purified Diet w/12% Energy From Fat, Yellow — 58G7

DESCRIPTION

Purified Laboratory Rodent Diet. Modification of TestDiet® 5755 with 12% energy from fat, dyed yellow.

Storage conditions are particularly critical to TestDiet® products, due to the absence of antioxidants or preservative agents. To provide maximum protection against possible changes during storage, store in a dry, cool location. Storage under refrigeration (2° C) is recommended. If long term studies are involved, store the diet at -20° C or colder. Be certain to keep in air tight containers.

*Product Forms Available**	*Catalog #*
1/2" Pellet	58145
1/2" Pellet, Irradiated	58168
Meal	1810736
Meal, Irradiated	1810737

**Other Forms Available By Request*

INGREDIENTS

Dextrin	50.1302
Casein - Vitamin Free	19.8700
Sucrose	15.0000
RP Mineral Mix #10 (adds 1.29% fiber)	4.7310
Corn Oil	4.7310
RP Vitamin Mix (adds 1.94% sucrose)	1.8924
Powdered Cellulose	1.4193
Inulin	1.4193
Lard	0.4257
Choline Chloride	0.1892
DL-Methionine	0.1419
Yellow Dye	0.0500

Part of the TestDiet® DIO Series

Basal Purified Diet with 45% Energy From Fat
1/2" Pellet - Catalog # 58146 (58G8)
Meal - Catalog # 58169 (58G8)

NUTRITIONAL PROFILE [1]

Protein, %	*17.6*
Arginine, %	0.69
Histidine, %	0.51
Isoleucine, %	0.95
Leucine, %	1.72
Lysine, %	1.44
Methionine, %	0.65
Cystine, %	0.07
Phenylalanine, %	0.95
Tyrosine, %	1.01
Threonine, %	0.77
Tryptophan, %	0.22
Valine, %	1.13
Alanine, %	0.55
Aspartic Acid, %	1.28
Glutamic Acid, %	4.06
Glycine, %	0.38
Proline, %	2.34
Serine, %	1.10
Taurine, %	0.00
Fat, %	*5.2*
Cholesterol, ppm	4
Linoleic Acid, %	2.75
Linolenic Acid, %	0.04
Arachidonic Acid, %	0.00
Omega-3 Fatty Acids, %	0.04
Total Saturated Fatty Acids, %	0.78
Total Monounsaturated Fatty Acids, %	1.32
Fiber (max), %	*3.9*
Carbohydrates, %	*68.3*
Energy (kcal/g) [2]	*3.85*

From:	kcal	%
Protein	0.705	18.3
Fat (ether extract)	0.464	12.1
Carbohydrates	2.733	71.0

Minerals	
Calcium, %	0.57
Phosphorus, %	0.54
Phosphorus (available), %	0.54
Potassium, %	0.38
Magnesium, %	0.07
Sodium, %	0.23
Chlorine, %	0.29
Fluorine, ppm	4.7
Iron, ppm	61
Zinc, ppm	26
Manganese, ppm	62
Copper, ppm	14.2
Cobalt, ppm	3.0
Iodine, ppm	0.54
Chromium, ppm	2.9
Molybdenum, ppm	0.77
Selenium, ppm	0.28

Vitamins	
Vitamin A, IU/g	20.9
Vitamin D-3 (added), IU/g	2.1
Vitamin E, IU/kg	47.4
Vitamin K (as menadione), ppm	9.84
Thiamin Hydrochloride, ppm	19.6
Riboflavin, ppm	19.6
Niacin, ppm	85
Pantothenic Acid, ppm	53
Folic Acid, ppm	3.9
Pyridoxine, ppm	15.6
Biotin, ppm	0.4
Vitamin B-12, mcg/kg	23
Choline Chloride, ppm	1,324
Ascorbic Acid, ppm	0.0

1. Formulation based on calculated values from the latest ingredient analysis information. Since nutrient composition of natural ingredients varies and some nutrient loss will occur due to manufacturing processes, analysis will differ accordingly. Nutrients expressed as percent of ration on an As Fed basis except where otherwise indicated.
2. Energy (kcal/gm) - Sum of decimal fractions of protein, fat and carbohydrate x 4,9,4 kcal/gm respectively

Table 1: Composition of standard diet.

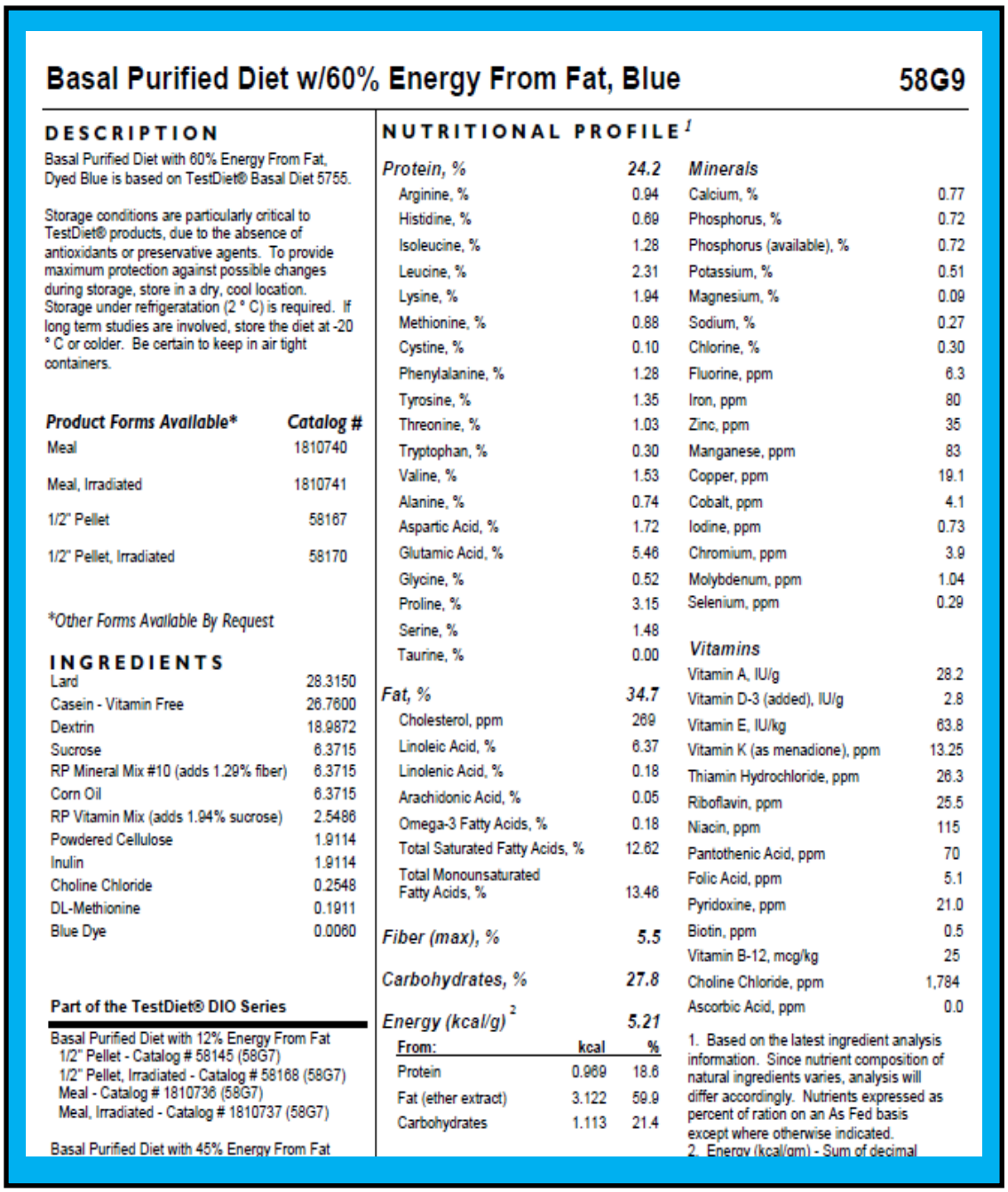

Basal Purified Diet w/60% Energy From Fat, Blue — 58G9

DESCRIPTION

Basal Purified Diet with 60% Energy From Fat, Dyed Blue is based on TestDiet® Basal Diet 5755.

Storage conditions are particularly critical to TestDiet® products, due to the absence of antioxidants or preservative agents. To provide maximum protection against possible changes during storage, store in a dry, cool location. Storage under refrigeratation (2 ° C) is required. If long term studies are involved, store the diet at -20 ° C or colder. Be certain to keep in air tight containers.

*Product Forms Available**	*Catalog #*
Meal	1810740
Meal, Irradiated	1810741
1/2" Pellet	58167
1/2" Pellet, Irradiated	58170

**Other Forms Available By Request*

INGREDIENTS

Lard	28.3150
Casein - Vitamin Free	26.7600
Dextrin	18.9872
Sucrose	6.3715
RP Mineral Mix #10 (adds 1.29% fiber)	6.3715
Corn Oil	6.3715
RP Vitamin Mix (adds 1.94% sucrose)	2.5486
Powdered Cellulose	1.9114
Inulin	1.9114
Choline Chloride	0.2548
DL-Methionine	0.1911
Blue Dye	0.0060

Part of the TestDiet® DIO Series

Basal Purified Diet with 12% Energy From Fat
1/2" Pellet - Catalog # 58145 (58G7)
1/2" Pellet, Irradiated - Catalog # 58168 (58G7)
Meal - Catalog # 1810736 (58G7)
Meal, Irradiated - Catalog # 1810737 (58G7)

Basal Purified Diet with 45% Energy From Fat

NUTRITIONAL PROFILE [1]

Protein, %	*24.2*
Arginine, %	0.94
Histidine, %	0.69
Isoleucine, %	1.28
Leucine, %	2.31
Lysine, %	1.94
Methionine, %	0.88
Cystine, %	0.10
Phenylalanine, %	1.28
Tyrosine, %	1.35
Threonine, %	1.03
Tryptophan, %	0.30
Valine, %	1.53
Alanine, %	0.74
Aspartic Acid, %	1.72
Glutamic Acid, %	5.46
Glycine, %	0.52
Proline, %	3.15
Serine, %	1.48
Taurine, %	0.00
Fat, %	*34.7*
Cholesterol, ppm	269
Linoleic Acid, %	6.37
Linolenic Acid, %	0.18
Arachidonic Acid, %	0.05
Omega-3 Fatty Acids, %	0.18
Total Saturated Fatty Acids, %	12.62
Total Monounsaturated Fatty Acids, %	13.46
Fiber (max), %	*5.5*
Carbohydrates, %	*27.8*
Energy (kcal/g) [2]	*5.21*

From:	kcal	%
Protein	0.969	18.6
Fat (ether extract)	3.122	59.9
Carbohydrates	1.113	21.4

Minerals	
Calcium, %	0.77
Phosphorus, %	0.72
Phosphorus (available), %	0.72
Potassium, %	0.51
Magnesium, %	0.09
Sodium, %	0.27
Chlorine, %	0.30
Fluorine, ppm	6.3
Iron, ppm	80
Zinc, ppm	35
Manganese, ppm	83
Copper, ppm	19.1
Cobalt, ppm	4.1
Iodine, ppm	0.73
Chromium, ppm	3.9
Molybdenum, ppm	1.04
Selenium, ppm	0.29
Vitamins	
Vitamin A, IU/g	28.2
Vitamin D-3 (added), IU/g	2.8
Vitamin E, IU/kg	63.8
Vitamin K (as menadione), ppm	13.25
Thiamin Hydrochloride, ppm	26.3
Riboflavin, ppm	25.5
Niacin, ppm	115
Pantothenic Acid, ppm	70
Folic Acid, ppm	5.1
Pyridoxine, ppm	21.0
Biotin, ppm	0.5
Vitamin B-12, mcg/kg	25
Choline Chloride, ppm	1,784
Ascorbic Acid, ppm	0.0

1. Based on the latest ingredient analysis information. Since nutrient composition of natural ingredients varies, analysis will differ accordingly. Nutrients expressed as percent of ration on an As Fed basis except where otherwise indicated.
2. Energy (kcal/gm) - Sum of decimal

Table 2: Composition of high fat diet

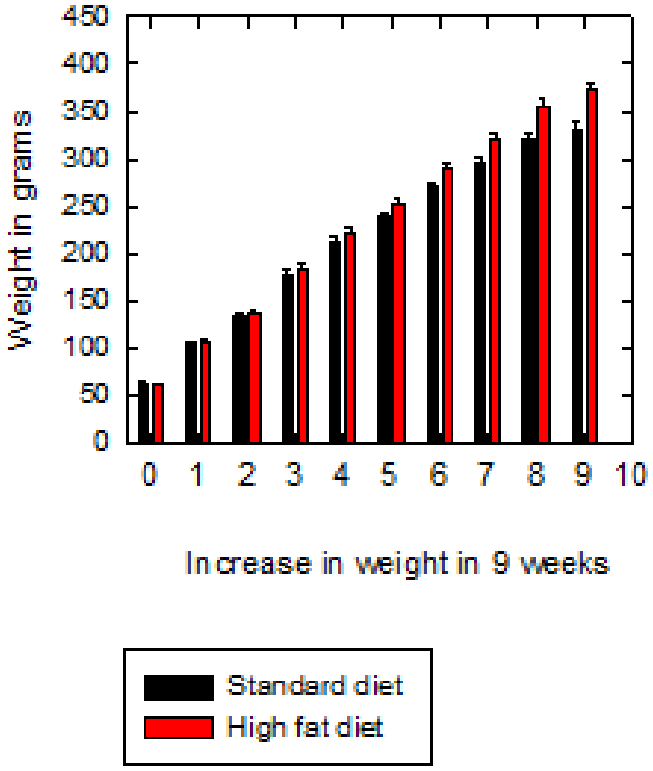

Fig 7: Weight: Four week old Sprague-Dawley rats were fed either control (black bars) or high fat (red bars) diets. Weight gain was measured weekly. n= 10

Table 3: Blood chemistry

Parameter	Control	High fat	P value
Weight (gms)	320 ± 6.899	354 ± 8.5	0.005
Albumin (g/dL)	4.3 ± 0.118	4 ± 0.0886	0.032
ALP (U/L)	167± 18	358 ± 25	≤ 0.001
ALT (U/L)	36 ± 2.3	40 ± 1.7	0.226
BUN (mg/dL)	15±0.7	16±0.9	0.474
Serum cholesterol(mg/dL)	95.6±7.7	112 ±4.3	0.073
Serum triglyceride(mg/dL)	91.2±11.8	67.1± 7.6	0.103
Serum HA	27.3±3.4	41.5±4.5	0.02
Serum bile acids (umol/L)	14.6 ± 4.9	13.2±2.7	0.793
Food consumed (Kcal)	50,712	57,440	
Serum free fatty acids (µmol/L)	153.75± 22.8	229±44	0.182 n = 4

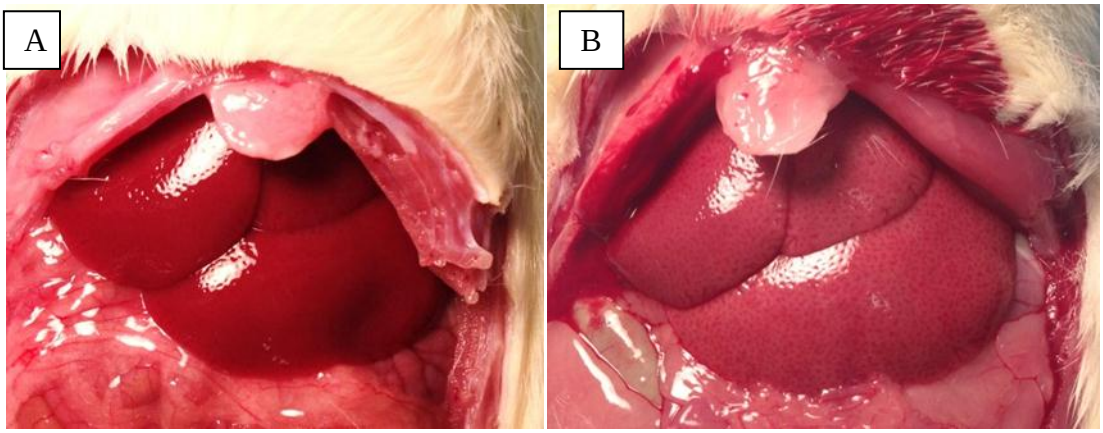

Fig. 8: Abdominal exposure and visual inspection of livers of rats fed (A) control and (B) high-fat diets. Increased fat deposition in the liver was often visible while the liver was extracted from an anesthetized live animal.

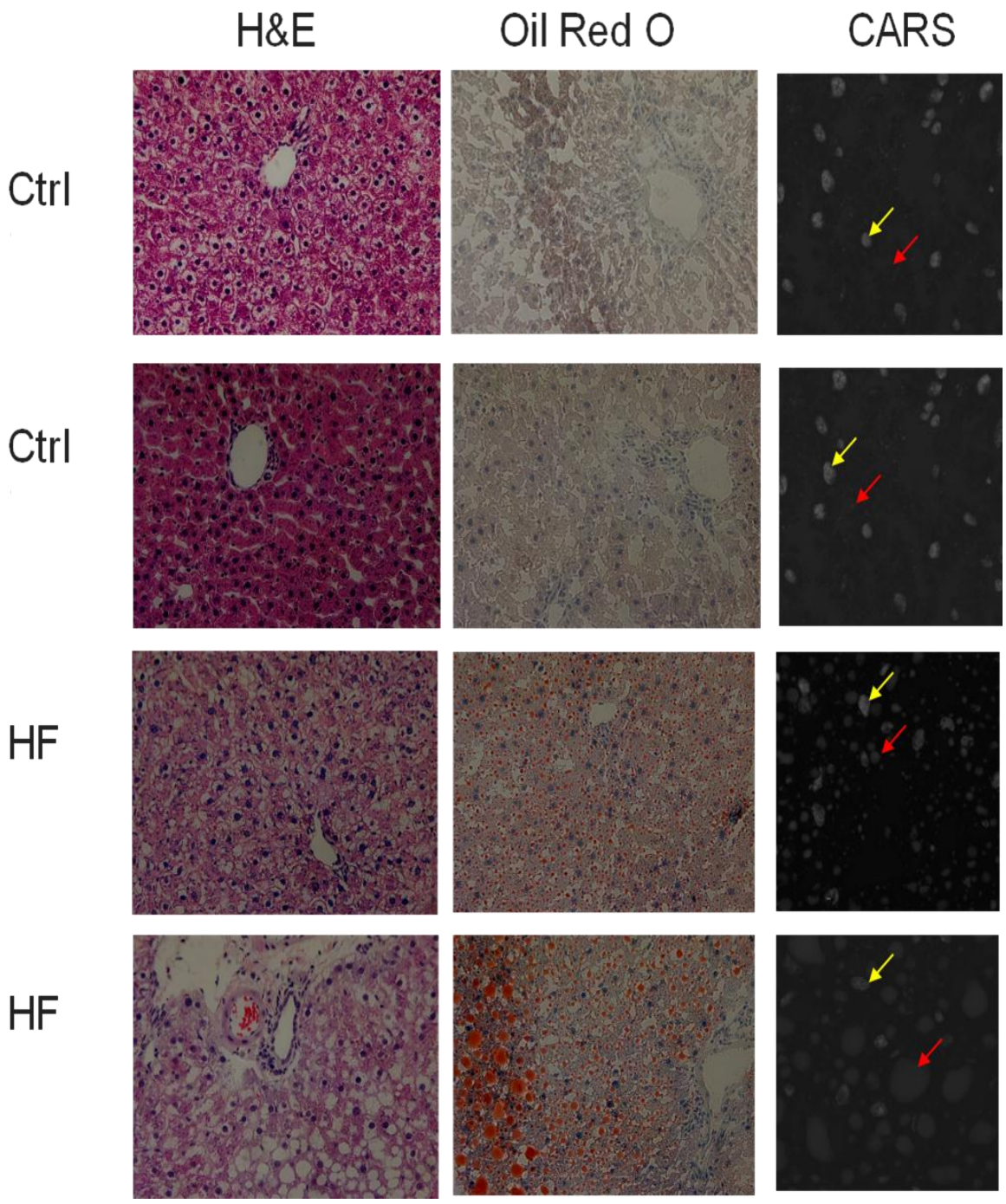

Fig 9: Liver tissues were sliced and then stained with H&E, or Oil Red O. Tissues slices were also subject to CARS microscopy to identify/confirm presence of fat droplets. Yellow arrows = nuclei stained with DAPI, Red Arrows = fat droplets.

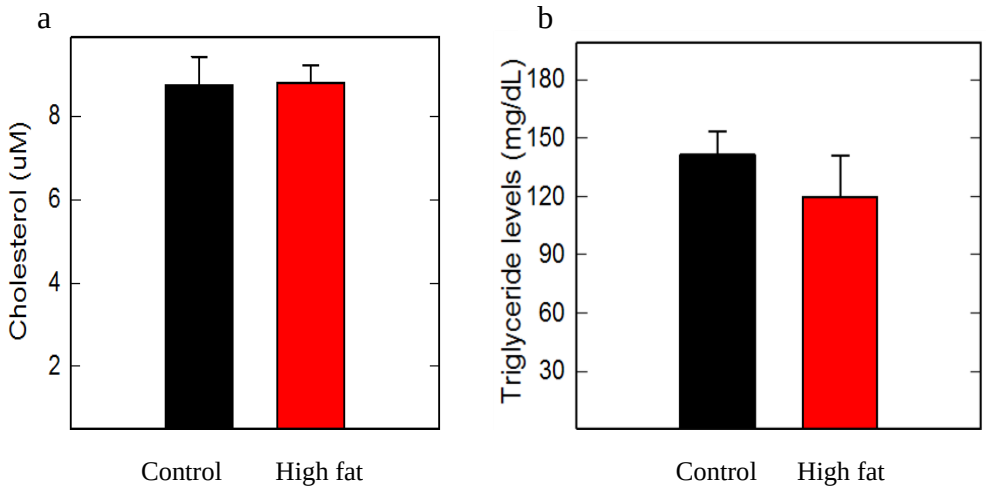

Fig 10: Blood chemistry a) Serum cholesterol levels, n= 10, p = 0.073, by t-test b) Serum triglyceride levels. n= 10, p = 0.103 , by t-test. Black bars are control rats and red bars indicate high fat rats.

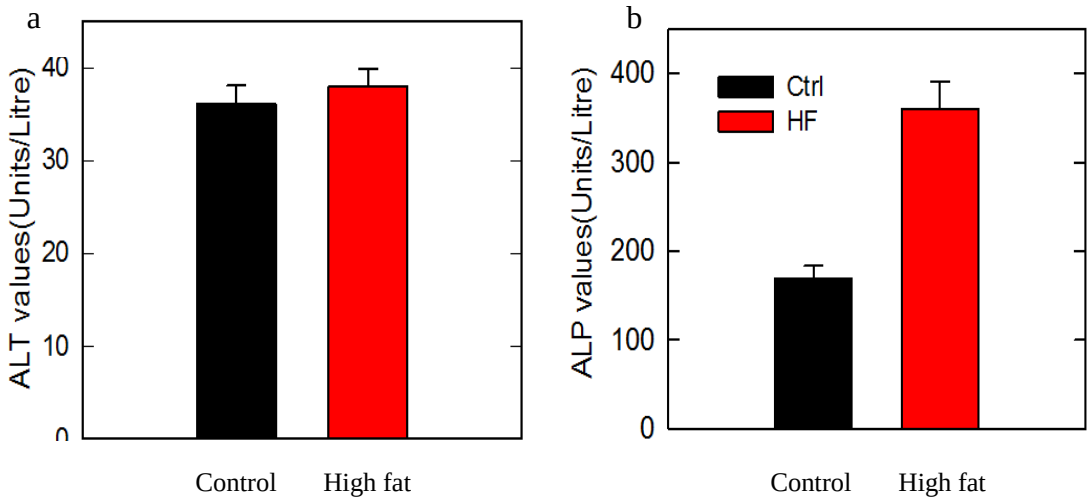

Fig 11: Liver enzymes values in control and high fat rats a) Alanine transaminase. n=1 0, p= 0.226 by t-test

b) Alkaline phosphatase levels. n= 10, $p \leq 0.001$, Black bars are control rats and red bars are high fat rats.

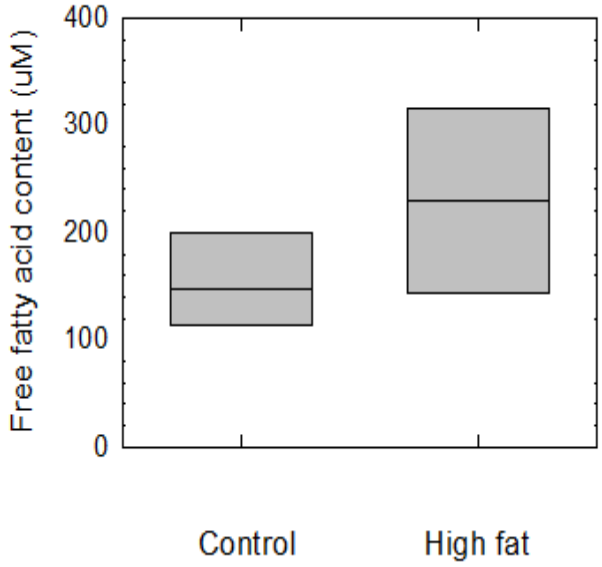

Fig 12: Serum free fatty acid assay. n = 4, p =0.182(t-test).

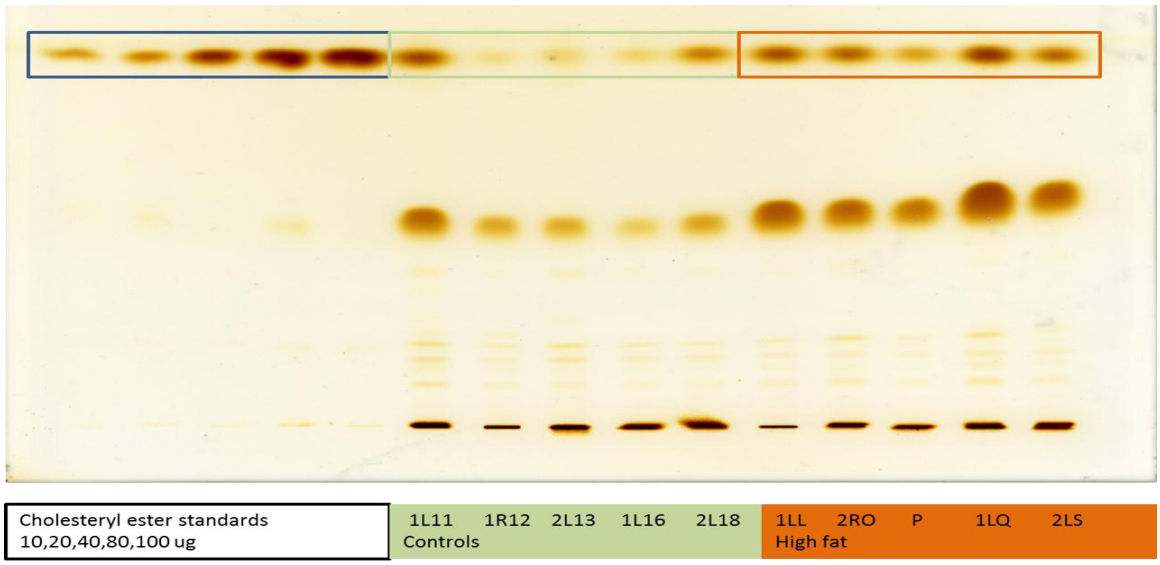

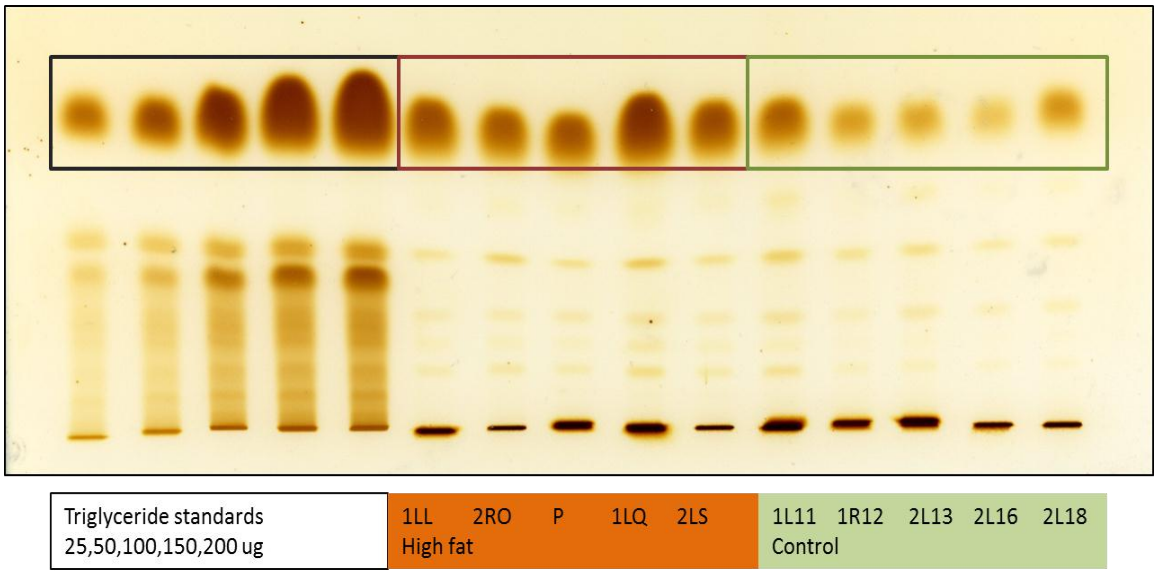

Fig 13: Lipid composition of liver tissue by Thin Layer Chromatography (TLC). Liver tissues (50 mg) from 5 rats in each group were processed for lipid content and prepared for TLC. Samples were spotted at the origins (arrows) and allowed to migrate up in a solvent (hexane, diethyl ether, acetic acid) saturated atmosphere. Plates were then stained with iodine vapor. Control 1L11,1R12,2L13,2L16,2L18 and High fat 1LL, 2RO, P, 1LQ and 2LS are the names of the control and high fat rats analyzed.

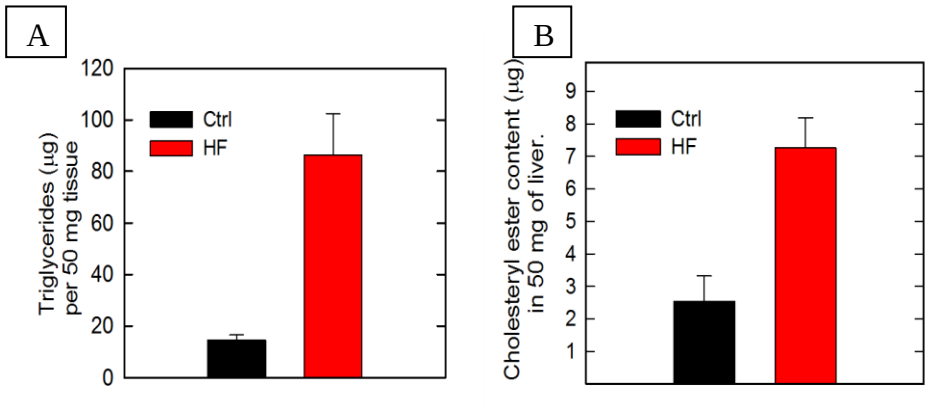

Fig. 14: Densitometry of TLC data. A) Triglyceride levels in liver. n=5, p=0.015 (t-test), b) Cholesteryl ester levels in liver . n= 5, p =0.007 Bands/spots of each control and HF groups were analyzed by ImageJ software and quantified.

CHAPTER 4

SINUSOIDAL ENDOTHELIAL DYSFUNCTION IN FATTY LIVER DISEASE

Chapter 4

Sinusoidal dysfunction in fatty liver disease

4.1 Introduction

Sinusoidal endothelial dysfunction in the liver is marked by capillarization or defenestration, which is defined as the loss of fenestrae and the development of basement membrane (58). The LSEC dysfunction results in decreased endocytic capability (94). Recent studies reveal the involvement of LSEC dysfunction in NAFLD. Sinusoidal endothelial cells are subject to insulin resistance in fatty liver disease. It has also been observed that sinusoidal endothelial dysfunction precedes inflammation and fibrosis in fatty liver disease (40, 67, 95). Currently, there are no studies that elucidate the role of the endocytic function of the LSECs in fatty liver disease.

Hyaluronic acid (HA) is a matrix polysaccharide with repeated disaccharide units of D-glucuronic acid and N-acetylglucosamine. HA is a major constituent of the ECM, and serum HA is known to be associated with inflammation, wound healing, and regenerative morphogenesis. Elimination of denatured or excess HA from the circulation is necessary to maintain the normal range of blood viscosity (96). Though many studies show the elevation of serum HA in NAFLD, the reason behind the elevation has been unexplained.

In our current study, the liver tissues were subjected to scanning electron microscopy to reveal the structural changes in the fenestrae. The isolated hepatocytes and LSEC were stained with Oil Red O, BODIPY stains and CARS microscopy was performed to observe the lipid accumulation in the cells. Serum HA was measured in the

control and HFD rats. LSECs isolated from control and HFD livers were plated on fibronectin-coated wells and assayed for ^{125}I-HA endocytosis. RNA isolated from the LSEC of the control and HFD rats were analyzed by micro-array analysis to study the expression of different genes in the LSEC.

4.2 Materials and methods

4.2.1 SEM of the liver

The rat was anesthetized and the procedure detailed in chapter 2 was followed until after the cannulation of the liver with a catheter. The liver was then flushed with TBS and perfused with fixation buffer (3% glutaraldehyde, 2.5% paraformaldehyde, 2mmol/L calcium chloride, 2% sucrose and 0.1 mol/L cacodylate buffer) at a constant perfusion rate of 10 mL/min for 10 minutes (97). The tissue is then isolated from the animal and cut into thin slices with a clean razor blade and stored in fixation buffer. The fixed tissues were then processed by the Microscopy Core Facility at UNL for scanning electron microscopy (SEM).

4.2.2 Staining of cells

The isolation of the cells of the liver was performed as described in chapter 2. The isolated hepatocytes and sinusoidal endothelial cells were stained with Oil Red O and BODIPY. CARS imaging was performed to visualize the lipid content in the cells. Oil Red O staining was performed in the following manner. The isolated hepatocytes were cultured in DMEM with 8% FBS and sinusoidal endothelial cells were cultured in RPMI containing 0.5% BSA for at least one hour. Media was removed from cultured plates, plates were rinsed with 5 mL phosphate buffered saline (PBS), and the cells were fixed

with 5 mL 4% buffered formalin for 15 min at room temperature. After 10 min, the formalin was discarded and fresh formalin was added and incubated for at least 1 hr, followed by 2 rinses with sterile water and subsequent 5 min incubation with 60% isopropanol. The isopropanol was removed and the cells were stained for 10 min with 5 ml of freshly diluted and filtered working Oil Red O solution (Working solution is 6 parts Oil Red O stock solution and 4 parts water). Oil red O stock solution is 0.35% oil red in 100% isopropanol. The stain was then removed and the cells were washed 5 times with sterile water. Images of cells stained with Oil Red O were obtained with a phase contrast microscope (98, 99).

The fluorophore BODIPY specifically stains neutral lipids. BODIPY staining was performed following the procedure as described previously (100). The cells were cultured on fibronectin-coated plastic chamber slides. They were rinsed with Dulbecco's phosphate buffered saline, fixed for 20 min with formaldehyde containing buffer (0.1 M PIPES pH 6.9, 1 mM EGTA, 3 mM MgSO4, 2.5% formaldehyde) and washed 3 times for 10 min with D-PBS before a short permeabilization with D-PBS + 0.1% triton X-100. The cells were washed with D-PBS following permeabilization and BODIPY was added on to the coverslips and incubated for 30 min. A 1 mg/mL BODIPY stock solution dissolved in DMSO was then diluted to 0.1 mg/ml and added to the cells. The slides were washed three times with D-PBS for 10 min each. Finally, coverslips were mounted using the UltraCruz mounting media. The cells were then observed under a fluorescent microscope (100).

4.2.3 CARS imaging

The isolated hepatocytes and LSEC were cultured on fibronectin-coated chamber slides for two hours and then fixed with 4% buffered formalin. The cells were visualized using CARS imaging at 2845 cm^{-1} with the assistance of Mr.Xiangnan He under the direction of Dr. Yongfeng Lu, Professor of Electrical Engineering at the University of Nebraska.

4.2.4 Measurement of serum Hyaluronate (HA)

The levels of HA in the serum from control and HFD rats were measured by ELISA using the Quantikine ELISA HA assay kit. The kit employs a solid phase ELISA to measure ≥ 35 kDa HA. It is a quantitative sandwich immunoassay method. The kit supplies a microplate onto which recombinant human (rh) Aggrecan, an HA binding protein has been pre-coated. Standards, controls, and samples were pipetted into the wells and any Hyaluronan present was bound by the immobilized rhAggrecan. After washing away any unbound substances, enzyme-linked rhAggrecan was added to the wells. It was followed by a wash to remove any unbound rhAggrecan-enzyme reagent and a substrate solution was added to the wells. The color development was stopped and measured. The intensity of color developed is in proportion to the amount of Hyaluronan bound in the initial step (Quantikine ELISA HA assay).

4.2.5 *In vitro* endocytosis of ^{125}I-HA

The isolated sinusoidal endothelial cells were cultured on fibronectin-coated 12-well plates in RPMI containing 0.05% BSA and allowed to recover for at least 90 min. Meanwhile two sets of endocytosis media (DMEM+0.05% BSA) containing 1) 1µg/ml

^{125}I-HA (hot) and 2) 1µg/mL ^{125}I -HA+ 100 µg/mL unlabeled HA (hot +cold) was prepared. After the cells are recovered, RPMI media was aspirated and the media containing either hot or hot+cold HA was added to the cells. The internalization of hot+cold HA by the cells served as a control to measure the specificity of HA uptake. The cells were allowed to internalize ^{125}I-HA for a period of 3 hours followed by three washes with HBSS (Hanks Buffered Salt Solution) and harvested using 0.5% NP-40. The radioactivity of the cell lysates was measured by gamma counter. The amount of radioactivity measured is proportional to the amount of ^{125}I-HA taken up by the cells. The protein content of the lysates was measured using Coomassie blue Bradford protein assay and the amount of ^{125}I- HA uptake is measured as CPM/mg protein (counts per minute/milligram protein).

4.2.6 Western blot of the LSEC lysates

The cells were lysed with 0.5% NP-40 containing protease inhibitors such as EDTA and PMSF. The lysates were spun briefly to settle any cell debris and the protein concentrations were measured using Coomassie blue Bradford protein assay method. Equal amounts of protein from the lysates was loaded on a 5% acrylamide gel and transferred to a nitrocellulose membrane after SDS-PAGE. The membrane was probed with anti-rat Stabilin-2 (Ab30) antibody and detected with anti-mouse antibody conjugated to horse radish peroxidase.

4.2.7 RNA isolation and microarray analysis

The isolated sinusoidal endothelial cells from replicates of control and HFD rats were stored in RNALater until utilized for RNA purification. RNA was isolated from the

replicates using the Trizol reagent (Life Technologies) followed by additional cleaning using an RNeasy kit (Qiagen). Microarray analysis was performed using Affymetrix Rat 1.0 gene chips at the Center for Bioinformatics and Systems Biology, University of Nebraska Medical Center, Omaha. The microarray results were used to identify potential genes that are either up- or down-regulated in the high fat diet regimen.

4.2.8 Analysis of Stab-2 gene expression by qPCR

RNA isolated from control and HFD rats were used for qPCR analysis of the difference in Stab-2 gene expression. Two different sets of primer pairs , 1) Stab-2 2771 For 5'-GAGGAAACGGGATTGACTGTGAACCCAT-3' and Stab-2 3590 rev 5'-ATGCCGTTATGCAAGTCATTCTTCAGGAG-3' , 2) Stab-2 3343 For 5'-TCTTTACCAAGTCTACTCACCCGTCTG-3' and Stab-2 Stab-2 3590 rev 5'-ATGCCGTTATGCAAGTCATTCTTCAGGAG-3' were used. cDNA synthesis was performed using Revertaid first strand cDNA synthesis kit(Fermentas). qPCR was performed using iTaq Universal SYBR Green Supermix (Biorad). The samples were run on ABI 7500 (Applied Biosystems) on the standard protocol. GAPDH gene was used for the reference gene expression. The change in expression was calculated using the ΔΔCt method.

4.3 Results

Staining of isolated hepatocytes from control and HFD rats showed considerable accumulation of fat in the hepatocytes in HFD rats as compared to the control (Fig 15). Staining of isolated sinusoidal endothelial cells reveals that these cells do not accumulate fats irrespective of the diet ingested (Fig 15). The scanning electron micrograph of the

liver tissue from the control and the HFD rats are not very different, though the fenestrations seems to be more disorganized in the HFD rats compared to the control (Fig 16). Serum HA is elevated in the HFD rats (Fig 17). The *in vitro* endocytosis of I-HA experiments show that the uptake of ^{125}I-HA is impaired in sinusoidal endothelial cells of the control rats compared to the HFD rats (Fig 18). The western blot of the lysates of the isolated LSEC culture of control and HFD rats show that the protein expression of Stab2 remains the same in both control and HFD rats (Fig 19). Densitometry measurements show that the amount of protein expressed is not significantly different through the microarray data show a downward trend (Table 4). qPCR analysis of Stab2 gene expression shows that there is 42 % decrease in expression in HFD rat livers compared to the control rats (Fig 20). A preliminary list of the genes revealed by microarray analysis to be up-regulated or down-regulated by the high fat diet is given (Table 3 and table 4). Different inflammatory response genes such as IL-6, Ccr1, Orm1, Vnn1, Olr1 and Ccl12 are upregulated, suggesting the role of stabilin-2 in inflammatory response to the high fat even before the fibrosis is set in. Other genes that are upregulated are Lbp, Ugt2b, Lox, Kng1, St8sia3, Lipc and LOC498793. Stabilin-1 and stabilin-2 are down regulated, but not to a significant level. qPCR analysis of the gene expression is required to give the exact fold change between the control and HFD rats.

4.4 Discussion

NAFLD is the major predictor for more serious health problems such as metabolic syndrome, hepatitis and cirrhosis. The sedentary lifestyle, in addition with the increased consumption of refined foods rich in fats and fructose is likely the reason for the proliferation of this disorder. It has been observed that a decrease in the consumption of

fatty refined foods and an increase in physical activity fully reverses NAFLD to normal healthy tissue (101). Though there are various studies that elucidate the effect of this metabolic disorder on the cells of the liver, the development of the disease is still very vague and requires more study. SEM of the liver reveals a change in the morphology of the fenestrae in the livers of the HFD rats. A decrease of the endocytic capability of the LSECs suggests that these cells are adversely affected during early stages of NAFLD. The staining of the isolated LSEC and hepatocyte helped identify that LSEC do not accumulate any fats suggesting that the direct effects of stored fatty acids (triglycerides) do not affect LSEC endocytosis directly, but that the effects of lipotoxicity may be in play.

The microarray results reveal certain genes of interest that are upregulated. Different inflammatory response genes such as IL-6, Ccr1, Orm1, Vnn1, Olr1 and Ccl12 are upregulated, suggesting the role of LSEC in inflammatory response to the high fat even before the fibrosis is set in. IL-6 is an interleukin and the circulating levels and expression of IL-6 is often found elevated in fatty liver disease (102). Ccl12 is a chemokine and is similar to Ccl2 and it is usually elevated along with other cytokines in NAFLD (103). Orm1 encodes for alpha-1 acid glycoprotein, also known as orosomucoid 1, whose expression is elevated as an acute immune response, has been observed to increase in hepatic steatosis (104).Vnn1 is an inflammatory response protein, which has been studied to be upregulated in fatty liver disease (105). Olr1 exhibits the activity of oxidized lipoprotein receptor, and is elevated as an inflammatory response. Though there is no literature pertaining to increased expression in NAFLD, Olr1 has been studied in relation to myocardial infarction (106). Other genes that are upregulated are Lbp, Ugt2b,

Lox, Kng1, St8sia3 and Lipc. Ugt2b belongs to the family of UDP-glucoronyl transferases, a group of enzymes involved in glucoronidation of toxic substances and aids in their removal. Drug metabolic alterations have been observed in NAFLD (107) and a study of the elevation of Ugt2b gene will provide a deeper understanding of the process in NAFLD. Lbp is lipopolysaccharide-binding protein and is found to be elevated in response to circulating endotoxin (108). Lox is lysyl oxidase and has been studied for its role in collagen fibril formation and fibrogenesis (109) and is being implicated as one of the genes in fatty liver disease in relation to fibrogenesis (110). Kng1 has been implicated in a positive role for endothelial cell proliferation and has been found to be one of the genes routinely over expressed in NAFLD (111). St8sia3 encodes for a protein involved in glycosphingolipid pathway and protein glycosylation (112). The relation between over expression of this gene and NAFLD has not yet been studied. Lipc encodes hepatic triglyceride lipase and has been studied in association with diabetes mellitus (113), but no relevant studies in relation to NAFLD have been carried out. Scd1 encodes for stearoyl-coA desaturase, which is a key enzymes in the synthesis of unsaturated fatty acid chains. There are various studies reporting the increase in expression of Scd1 in the livers in fatty liver disease (114-116), though we have observed that the expression of Scd1 is down regulated in LSEC. An in-depth analysis of genes in other lipid metabolic pathways is required to understand the downward trend in expression of Scd1 observed in LSEC. We observed that expression of stabilin-1 and stabilin-2 are down-regulated as seen by microarray analysis, and stab2 gene expression is decreased by 42 % as validated by qPCR.

Elevated serum HA levels are in agreement with the decreased LSEC endocytosis rate, while receptor levels are unchanged indicating that endocytic machinery for receptor internalization may be impaired. These studies along with the investigation of what LSEC genes are affected by the high fat diet open avenues for understanding the role of LSEC in early events of NAFLD.

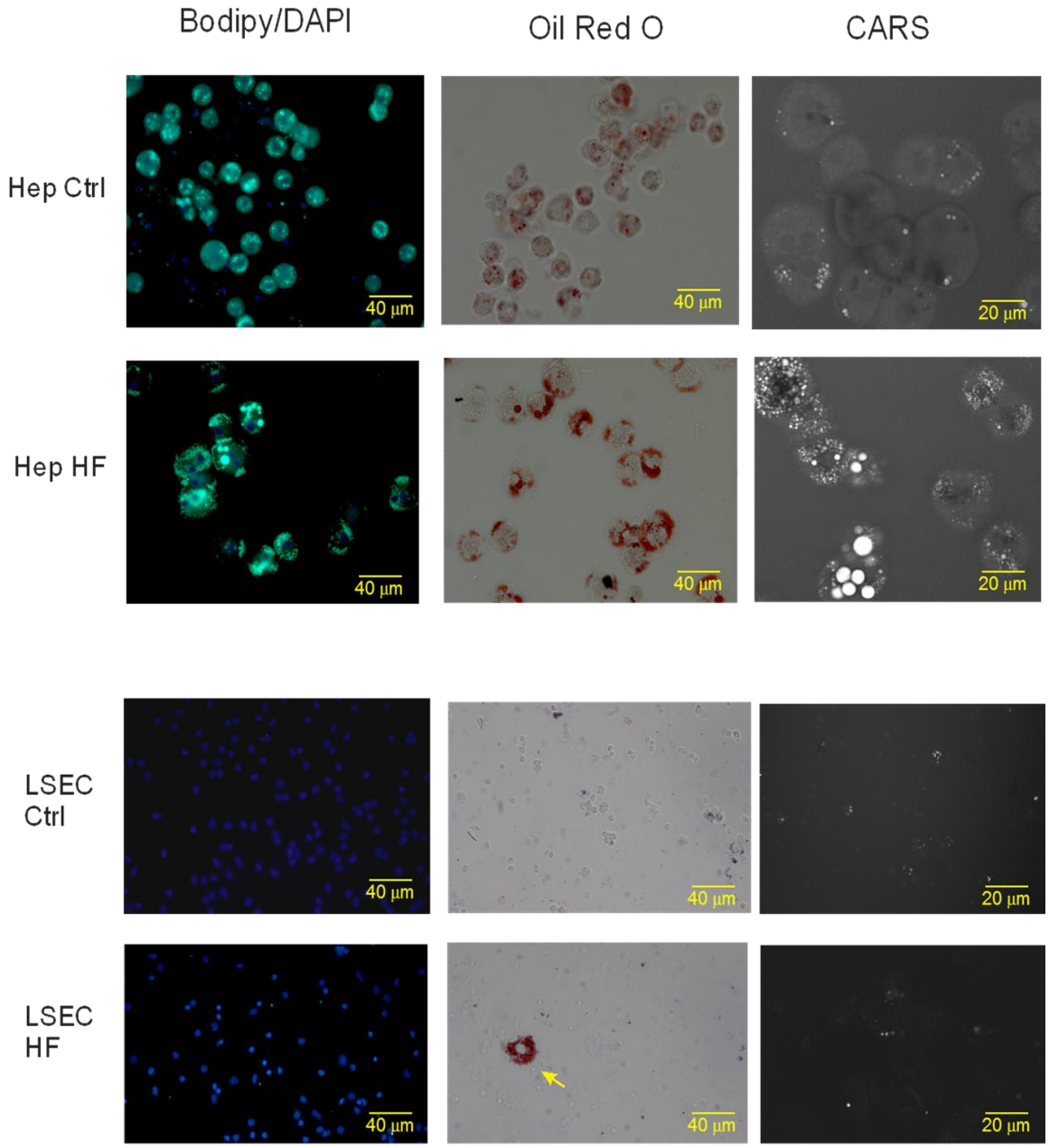

Fig 15: Isolated hepatocytes and LSEC as viewed by either BODIPY staining, Oil Red O staining, or Coherent Anti-Stokes Raman Scattering (CARS) Microscopy. BODIPY stains fat droplets in the fluorescent green wavelength (Ex 495:Em 519), Oil Red O stains fat droplets red under PC light microscopy, and CARS microscopy at 2845 cm^{-1} for CH_2 symmetric stretching vibration. Yellow arrow shows distinction of a single hepatocyte in a large group of LSEC stained with Oil Red O. SEC do NOT store fats

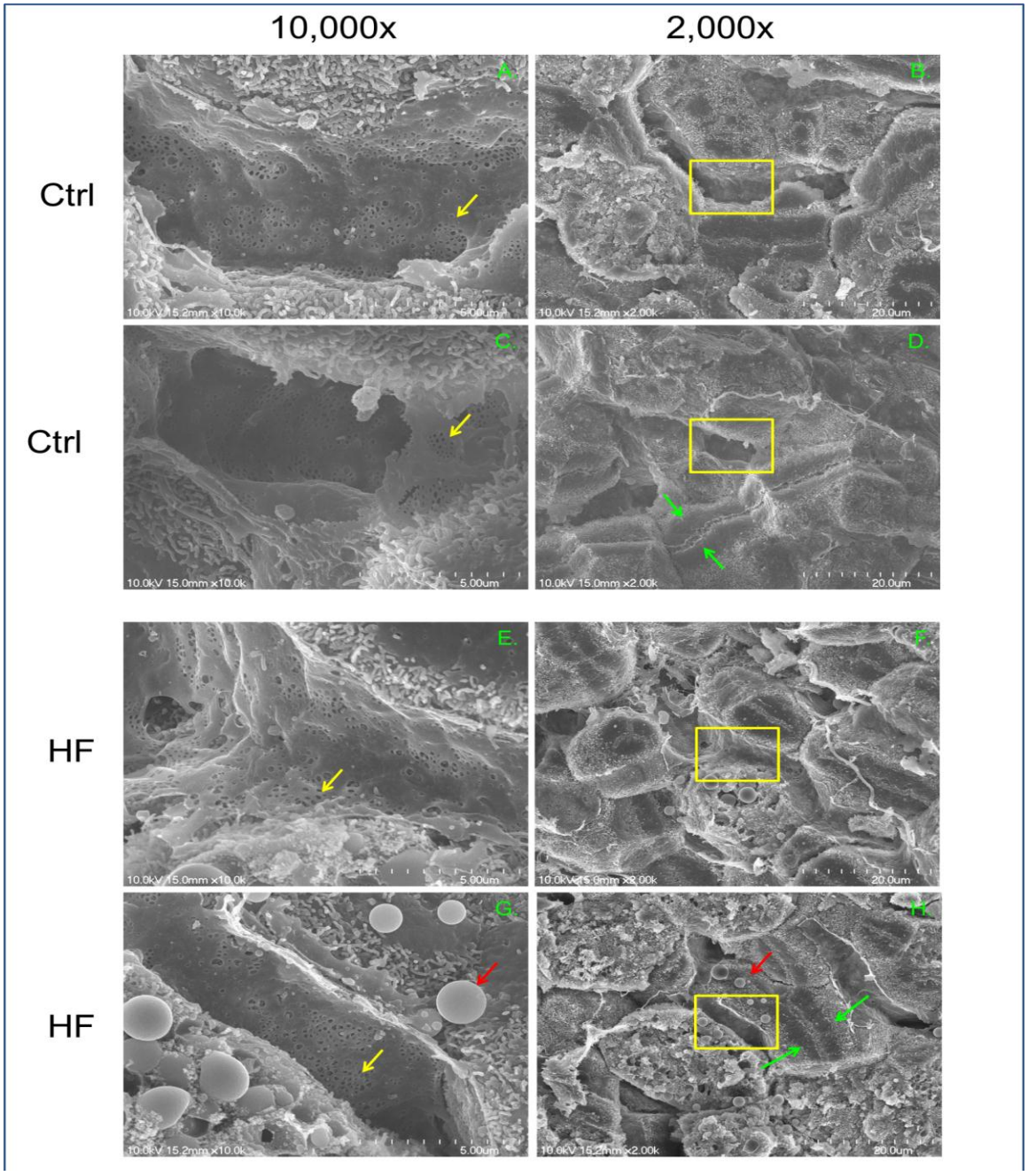

Fig 16: SEM micrographs of livers from rats fed control (A-D) and HF diets (E-H). Fenestration (yellow arrows) in the LSEC of both groups is in good condition although a little more disorganized in the HF group. The green arrows point to adjacent hepatocytes between the sinusoidal vessels and the red arrows show fat droplets that originated in the hepatocytes. The spherical shapes in G and H are displaced lipid droplets.

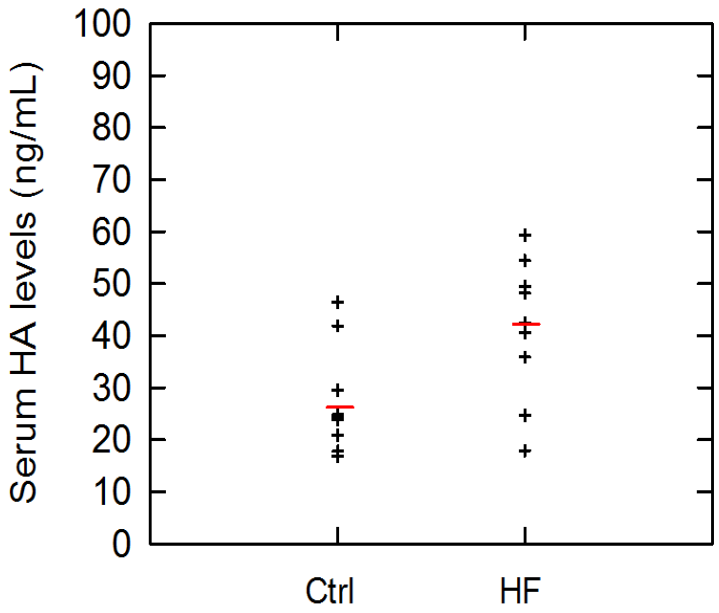

Fig 17: Serum HA levels were measured from both control and HFD rats using the Quantikine ELISA HA assay kit (R &D systems). Each data point represents an animal with the red bars indicating the mean, n=9, p = 0.02 by t-test.

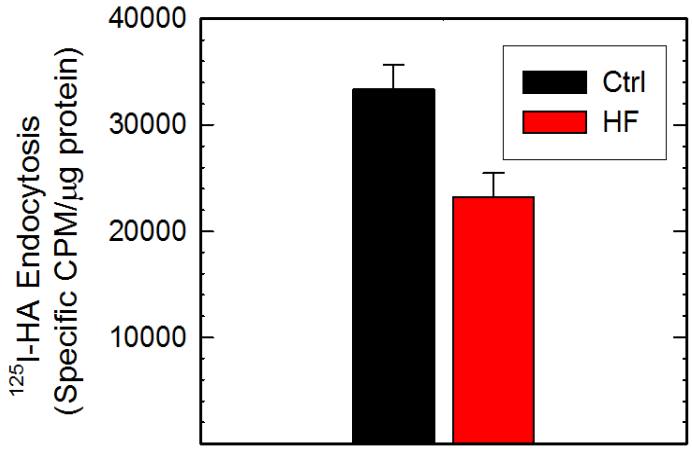

Fig 18: In vitro endocytosis; LSEC isolated from control and HFD livers were plated on fibronectin-coated plate, recovered for 2 hours and then allowed to internalize ^{125}I-HA for 3 hours. Cells were then washed and measured for radioactivity and protein levels. n=4, p= 0.018, by t-test.

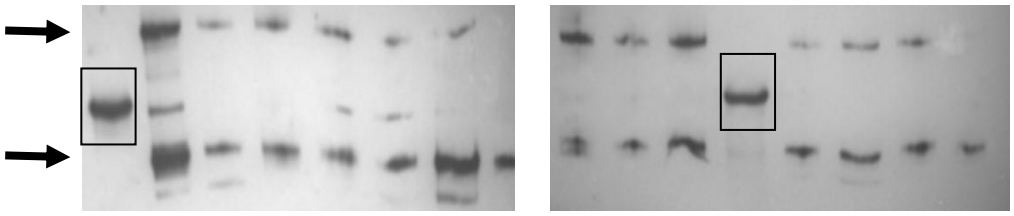

Control rats High fat rats

Fig 19: Western blot of LSEC lysates from control and HFD rats. The proteins were probed with Stabilin-2 antibody (Ab30). The two arrows correspond to the two isoforms of stabilin-2 protein (300 and 170 kd). The black boxes indicate the marker of 250 kd.

Table 4 Summary list of genes upregulated

Gene	High fat /Control	Function
IL-6	1.86	Interleukin
Ccr1	1.79	Chemokine receptor
Orm1	2.7	Orosomucoid 1
Vnn1	2.1	Vanin 1
Olr1	1.99	Oxidative low density lipoprotein receptor 1
Ccl12	2.03	Cytokine
Lbp	2.17	Lipopolysachcharide binding protein
Ugt2b	2.84	UDP-glucoronyl transferase family
Lox	2.83	Lysyl oxidase
Kng1	2.56	Kininogen 1
St8sia3	2.27	alpha2-8 sialyltransferase.
Lipc	1.93	Hepatic lipase

Table 5 Summary list of genes down regulated

Gene	High fat/Control	Function
Scd1	0.3	Stearoyl CoA desaturase.
Stabilin-1	0.65	Scavenger receptor
Stabilin-2	0.66	Scavenger receptor

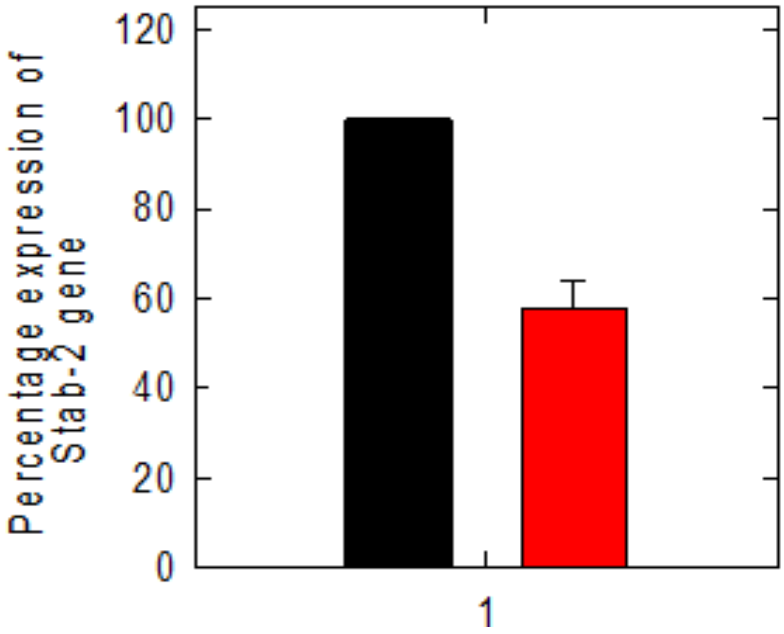

Fig 20: qPCR analysis of Stab-2 gene expression. n= 3, $p \leq 0.001$(t-test).

CHAPTER 5

CONCLUSIONS AND FUTURE DIRECTIONS

Chapter 5

Conclusions and Future Directions

The pathogenesis of NAFLD is not yet clear and there is an on-going search for specific serum markers that help diagnose NAFLD. Though there are various research studies to elucidate the effect of fatty liver on the different cells of the liver, sufficient research into the role of liver sinusoidal endothelial cells (LSEC) in the pathogenesis of the disease has not been done. The LSEC act as a liver sieve by allowing macromolecules and chylomicrons to traverse through their fenestrations (sieve plates) to hepatocytes (58). Since LSEC regulate serum-derived macromolecular exposure to hepatocytes, we asked what role LSECs play in the pathogenesis of NAFLD. Two sets of rats were maintained on standard and high fat diets (HFD) respectively for a period of 8 weeks. The lipid accumulation in the rat livers, isolated hepatocytes and LSEC were visualized by Oil Red O, BODIPY and CARS imaging. These analyses reveal the accumulation of lipid droplets in the hepatocytes of HFD fed rats in contrast to the LSECs. These studies reveal that the LSEC do not accumulate fat due to the high fat diet and do not respond to the diet in a similar fashion as the hepatocytes. We carried out *in vitro* endocytosis of ^{125}I-HA that showed ^{125}I-HA uptake is significantly higher in isolated SEC of control rats compared to HFD fed rats, as measured by statistical analyses using t-test. We also observed that serum hyaluronate (HA) levels and alkaline phosphatase (ALP) levels were increased in HFD fed rats, in contrast to alanine transaminase (ALT), triglycerides and cholesterol, which remained the same. Though the fasting serum triglyceride levels of the HFD were not significantly different from the control rats, thin layer chromatography of the lipid extracts of the liver tissues from the HFD and control rats showed a significantly

higher amount of triglycerides and cholesteryl ester in the HFD rats compared to the control rats, as measured by statistical analyses using t-test. All these experiments established that the rats fed on HFD were suffering from fatty liver disease after 8 weeks of high fat food consumption.

The most significant observation of the study so far has been the decreased uptake of hyaluronate (HA) by the isolated SEC. Serum HA is also significantly high in the HFD rats compared to the control. Serum HA has also been observed to be elevated in various diseased conditions including diabetes mellitus (117), liver hepatitis and cirrhosis (118) and hepato-cellular carcinoma (119), but the reason for the elevated serum HA in these conditions has not been elucidated.

The Stabilin-2 receptor is the only receptor on the SEC that is responsible for the clearance of HA (26) and other matrix material. The decrease in uptake of HA in the livers of HFD rats suggests the impairment of protein function, which could be either due to the decreased production of the protein, the decreased expression of the stabilin-2 gene or a malfunction in the endocytic pathway. The Stabilin-2 protein expression was measured by performing a western blot using the isolated LSEC culture lysates. The study revealed that there is no difference in the protein expression between the control and HFD rats. RNA was isolated from the LSECs of the control and HFD rats and subjected to microarray analysis, which revealed that the stabilin-2 gene expression was not changed between the control and HFD rats. Post-translational modification of stabilin-2 might be a reason for its decreased endocytic capability in the HFD fed rats.

Insulin resistance plays a role in the pathogenesis of liver damage in fatty liver disease (120). Some studies also suggest that both of them have a common pathogenic mechanism (121). Insulin resistance and hyper glycemic conditions results in activation of four pathways, the Protein Kinase C/Diacyl Glycerol pathway (PKC/DAG), the sorbitol pathway, the hexosamine pathway and the formation of advanced glycation end products (AGE) (122). The hexosamine pathway results in the channeling of fructose-6-phosphate to GlcNAC (N-Acetyl glucosamine). The increased production of GlcNAC results in post translation attachment of O-GlcNAC to serine and threonine residues of proteins, resulting in their inactivation (123). As there is an evidence that serine-2497 on the cytoplasmic side of the Stab-2 protein is phosphorylated and activated by phosphorylation (unpublished data), it will be interesting to see if the protein undergoes post translational O-GlcNAC attachment due to hyperglycemia and insulin resistance.

Insulin promotes nitric oxide (NO) production through the activation of the PI3K/Akt/endothelial nitric oxide synthase (eNOS) signaling pathway. The phosphorylation of eNOS at Serine 1179 results in vasodilatation and vascular protection. When insulin resistance develops, the PI3K pathway is inhibited and the PKC/DAG pathway is initiated. The PKC/DAG pathway is known to decrease eNOS activity (124). Hyperglycemia also results in mitochondrial dysfunction, which results in increased superoxide production (125). The superoxides result in the production of reactive peroxynitrite species which uncouple and inactivate eNOS by binding to tetrahydrobiopterin which is an essential cofactor for eNOS activity, resulting in production of more reactive species instead of NO (126). Hepatocytes have been shown to increase the production of inducible nitric oxide synthase (iNOS) as an inflammatory

response due to high fat diet. iNOS is known to cause insulin resistance by S-nitrosylation of the insulin signaling proteins (126).

The response of the LSEC to hyperglycemic conditions is still being studied. LSEC undergo insulin resistance due to hyperglycemic conditions in fatty liver disease and it precedes fibrosis and inflammation. This study is based on the decrease of Akt phosphorylation and eNOS in the liver, *in vivo* hemodynamic studies and decrease in vasodilatation (95). Another study by the same group suggests that iNOS production is increased in the hepatocytes due to high fat diet, which induces insulin resistance in sinusoidal endothelial cells, measured by in situ liver perfusion and hemodynamic studies. It is not clear how isolated LSECs respond (67). In steatosis, it has also been observed that the sinusoidal narrowing takes place and there is a decrease in sinusoidal flow (127). *In situ* assessment reveals an increase in portal pressure and intra hepatic resistance due to impaired sinusoidal endothelial function. An increase in vasoconstrictors and morphological disorganization was observed which precedes inflammation and fibrosis (128).

It will be beneficial to study the effect of insulin on the isolated LSEC, by exposing it to insulin and performing a pathway array analysis to study which proteins are being activated/deactivated due to insulin exposure in both control and HFD rat LSEC. The study of the changes in gene expression in the proteins in the insulin signaling pathway by qPCR will reveal the changes in the gene expression in the cells due to hyperglycemia and insulin resistance. Potential candidate genes are the class of Insulin receptors, eNOS, O-GlcNAC transferase, and inflammatory cytokines such as IL-6, TNF and TGF-β. The effect of insulin resistance needs to be observed in isolated LSEC,

paying special attention to the hexosamine pathway and the production of O-GlcNAC. Mass spectrometric studies of the Stabilin-2 protein will reveal if there is a post translation attachment of O-GlcNAC due to insulin resistance.

The liver sinusoidal endothelium undergoes changes in its unique phenotype and undergoes the process known as capillarization, which is the loss of LSEC fenestration and development of basement membrane (56). Capillarization has been known to occur in NAFLD and seen to precede onset of fibrosis (129). LSEC fenestrae are maintained by VEGF production by hepatocytes and consequent activation of eNOS by the endothelial cells (130). It has been observed in a previous study that LSEC differentiation plays a role in the fibrogenesis. LSEC differentiation promotes quiescence of hepatic stellate cells (HSC) and thereby promotes regression and inhibits progression of liver fibrosis (57). It has also been observed that the endocytic activity of the LSEC is reduced due to capillarization (59). All the above observations can be used to draw the following hypothesis that high fat diet causes the hepatocytes to produce more iNOS that cause insulin resistance in the endothelial cells and subsequent dysfunction.

The insulin resistance in the LSECs causes it to decrease the eNOS activity, which causes capillarization. The loss of the phenotype of the LSEC results in the activation of stellate cells and the fibrogenesis of the liver. The insulin resistance might also cause the O-GlcNAC addition on the stabilin-2 receptors that lose their ability to clear HA and other molecules. An insight into the HA secretion and degradation is necessary to establish the link between the increase in serum HA in liver damage and sinusoidal endothelial dysfunction.

Alkaline phosphatase is one of the liver enzymes studied to diagnose liver disease condition, the other two being the aspartate and alanine aminotransferases. Alkaline phosphatase is elevated in conditions of hepato-cellular damage and biliary obstruction. The expression of this enzyme is increased slightly in hepato-cellular damage, and induced to elevated levels and made into soluble forms especially when the bile ducts are obstructed (131). This could suggest a possible mechanism where the ductules are affected. It has also been observed that the alkaline phosphatase levels are increased in fatty liver disease even though there is no significant increase in triglyceride levels in the serum, (132). Our experiments also revealed similar observations. Even though rats do not have a gall bladder, bile is produced by the hepatocytes and secreted into bile ducts (92). It has also been observed that biliary obstruction results in decreased endocytic activity in hepatocytes and sinusoidal endothelial cells (93). An investigation between the sinusoidal endothelial dysfunction and the biliary obstruction is required.

Advanced glycation endproducts (AGE) products are seen to be elevated in NAFLD (133). The Stab-2 receptor is also involved in the removal of AGE products, as mentioned previously (29). It is not yet known if the isolated LSECs from HFD rats have a difference in their ability to remove AGE products, compared to the control diet rats. It has also been observed that the pre-exposure of the sinusoidal endothelial cells to AGE can result in decreased endocytic ability of the cells (134). The relation between elevated AGE and sinusoidal endothelial dysfunction in NAFLD has not yet been explored.

Chronic kidney failure is often associated with NAFLD (135). Deficiency of the Stabilin receptors in the liver results in glomerular nephritis of the kidney due to ECM buildup in the glomeruli (136). The link between NAFLD and chronic kidney failure

because of sinusoidal endothelial dysfunction is not yet known. As the study of the pathogenesis of NAFLD is a vast field, with new research observations coming in with each study, the above suggestions will provide a preliminary understanding of the role of LSEC in the pathogenesis of NAFLD. There are still many unknown molecular events in the initial stages of NAFLD development and pathogenesis.

REFERENCES

1. Arias IM, Boyer JL, Chisari FV, Arias, Boyer, Chisari, et al. The liver: Biology and pathobiology. Lippincott Williams & Wilkins Philadelphia PA; 2001.

2. Medlock ES, Haar JL. The liver hemopoietic environment: I. developing hepatocytes and their role in fetal hemopoiesis. Anat Rec. 2005;207(1):31-4.

3. Arii S, Imamura M. Physiological role of sinusoidal endothelial cells and kupffer cells and their implication in the pathogenesis of liver injury. J Hepatobiliary Pancreat. 2000;7(1):40-8.

4. Reinders ME, van Wagensveld BA, van Gulik TM, Corssmit NPM, Frederiks WM, Chamuleau RAFM, et al. No attenuation of ischemic and reperfusion injury in kupffer cell-depleted, cold-preserved rat livers. Transplantation. 1997;63(3):449-54.

5. Smedsrød B, De Bleser P, Braet F, Lovisetti P, Vanderkerken K, Wisse E, et al. Cell biology of liver endothelial and kupffer cells. Gut. 1994;35(11):1509-16.

6. Friedman SL. Hepatic stellate cells: Protean, multifunctional, and enigmatic cells of the liver. Physiol Rev. 2008;88(1):125-72.

7. Strazzabosco M. The cholangiopathies: Disorders of biliary epithelia. Gastroenterology. 2004;127(5):1565-77.

8. Masyuk AI, Masyuk TV, LaRusso NF. Cholangiocyte primary cilia in liver health and disease. Developmental Dynamics. 2008;237(8):2007-12.

9. Stolz DB. Sinusoidal endothelial cells. Molecular Pathology of Liver Diseases. 2011:97-107.

10. Wisse E. An electron microscopic study of the fenestrated endothelial lining of rat liver sinusoids. J Ultrastruct Res. 1970;31(1):125-50.

11. Knolle PA. Role and function of liver sinusoidal endothelial cells. Liver Immunology. 2007:25-39.

12. Braet F, Wisse E. Structural and functional aspects of liver sinusoidal endothelial cell fenestrae: A review. Comp Hepatol. 2002;1(1):1.

13. DeLeve LD, Wang X, Hu L, McCuskey MK, McCuskey RS. Rat liver sinusoidal endothelial cell phenotype is maintained by paracrine and autocrine regulation. American Journal of Physiology-Gastrointestinal and Liver Physiology. 2004;287(4):G757-63.

14. Esser S, Wolburg K, Wolburg H, Breier G, Kurzchalia T, Risau W. Vascular endothelial growth factor induces endothelial fenestrations in vitro. J Cell Biol. 1998;140(4):947-59.

15. Mori T, Okanoue T, Sawa Y, Hori N, Ohta M, Kagawa K. Defenestration of the sinusoidal endothelial cell in a rat model of cirrhosis. Hepatology. 2005;17(5):891-7.

16. Steffan AM, Pereira CA, Bingen A, Valle M, Martin JP, Koehren F, et al. Mouse hepatitis virus type 3 infection provokes a decrease in the number of sinusoidal endothelial cell fenestrae both in vivo and in vitro. Hepatology. 1995;22(2):395-401.

17. Xu B, Broome U, Uzunel M, Nava S, Ge X, Kumagai-Braesch M, et al. Capillarization of hepatic sinusoid by liver endothelial cell-reactive autoantibodies in patients with cirrhosis and chronic hepatitis. The American journal of pathology. 2003;163(4):1275-89.

18. Dobbs B, Rogers G, Xing H, Fraser R. Endotoxin-induced defenestration of the hepatic sinusoidal endothelium: A factor in the pathogenesis of cirrhosis? Liver. 1994;14(5):230-3.

19. Fraser R, Dobbs BR, Rogers GWT. Lipoproteins and the liver sieve: The role of the fenestrated sinusoidal endothelium in lipoprotein metabolism, atherosclerosis, and cirrhosis. Hepatology. 1995;21(3):863-74.

20. Popescu D, Movileanu L, Ion S, Flonta ML. Hydrodynamic effects on the solute transport across endothelial pores and hepatocyte membranes. Phys Med Biol. 2000;45(11):N157.

21. Wack KE, Ross MA, Zegarra V, Sysko LR, Watkins SC, Stolz DB. Sinusoidal ultrastructure evaluated during the revascularization of regenerating rat liver. Hepatology. 2003;33(2):363-78.

22. Funyu J, Mochida S, Inao M, Matsui A, Fujiwara K. VEGF can act as vascular permeability factor in the hepatic sinusoids through upregulation of porosity of endothelial cells. Biochem Biophys Res Commun. 2001;280(2):481-5.

23. Yokomori H, Oda M, Ogi M, Sakai K, Ishii H. Enhanced expression of endothelial nitric oxide synthase and caveolin-1 in human cirrhosis. Liver. 2009;22(2):150-8.

24. Le Couteur DG, Warren A, Cogger VC, Smedsrød B, Sørensen KK, De Cabo R, et al. Old age and the hepatic sinusoid. The Anatomical Record: Advances in Integrative Anatomy and Evolutionary Biology. 2008;291(6):672-83.

25. Elvevold K, Smedsrød B, Martinez I. The liver sinusoidal endothelial cell: A cell type of controversial and confusing identity. American Journal of Physiology-Gastrointestinal and Liver Physiology. 2008;294(2):G391-400.

26. McGARY CT, Raja R, Weigel PH. Endocytosis of hyaluronic acid by rat liver endothelial cells. evidence for receptor recycling. Biochem J. 1989;257(3):875.

27. Magnusson S, Berg T. Extremely rapid endocytosis mediated by the mannose receptor of sinusoidal endothelial rat liver cells. Biochem J. 1989;257(3):651.

28. Mousavi SA, Sporstøl M, Fladeby C, Kjeken R, Barois N, Berg T. Receptor-mediated endocytosis of immune complexes in rat liver sinusoidal endothelial cells is mediated by FcγRIIb2. Hepatology. 2007;46(3):871-84.

29. Tamura Y, Adachi H, Osuga J, Ohashi K, Yahagi N, Sekiya M, et al. FEEL-1 and FEEL-2 are endocytic receptors for advanced glycation end products. J Biol Chem. 2003;278(15):12613-7.

30. Li R, Oteiza A, Sørensen KK, McCourt P, Olsen R, Smedsrød B, et al. Role of liver sinusoidal endothelial cells and stabilins in elimination of oxidized low-density lipoproteins. American Journal of Physiology-Gastrointestinal and Liver Physiology. 2011;300(1):G71-8.

31. Smedsrod B. Clearance function of scavenger endothelial cells. Comp Hepatol. 2004;3(Suppl 1):S22.

32. Goerdt S, Walsh LJ, Murphy GF, Pober JS. Identification of a novel high molecular weight protein preferentially expressed by sinusoidal endothelial cells in normal human tissues. J Cell Biol. 1991;113(6):1425-37.

33. Prevo R, Banerji S, Ni J, Jackson DG. Rapid plasma membrane-endosomal trafficking of the lymph node sinus and high endothelial venule scavenger receptor/homing receptor stabilin-1 (FEEL-1/CLEVER-1). J Biol Chem. 2004;279(50):52580-92.

34. Kzhyshkowska J, Workman G, Cardó-Vila M, Arap W, Pasqualini R, Gratchev A, et al. Novel function of alternatively activated macrophages: Stabilin-1-mediated clearance of SPARC. The Journal of Immunology. 2006;176(10):5825-32.

35. Kzhyshkowska J, Gratchev A, Schmuttermaier C, Brundiers H, Krusell L, Mamidi S, et al. Alternatively activated macrophages regulate extracellular levels of the hormone placental lactogen via receptor-mediated uptake and transcytosis. The Journal of Immunology. 2008;180(5):3028-37.

36. Politz O, Gratchev A, McCourt PAG, Schledzewski K, Guillot P, Johansson S, et al. Stabilin-1 and-2 constitute a novel family of fasciclin-like hyaluronan receptor homologues. Biochem J. 2002;362(Pt 1):155.

37. Park SY, Jung MY, Lee SJ, Kang KB, Gratchev A, Riabov V, et al. Stabilin-1 mediates phosphatidylserine-dependent clearance of cell corpses in alternatively activated macrophages. J Cell Sci. 2009;122(18):3365-73.

38. Adachi H, Tsujimoto M. FEEL-1, a novel scavenger receptor with in vitro bacteria-binding and angiogenesis-modulating activities. J Biol Chem. 2002;277(37):34264-70.

39. Karikoski M, Irjala H, Maksimow M, Miiluniemi M, Granfors K, Hernesniemi S, et al. Clever-1/Stabilin-1 regulates lymphocyte migration within lymphatics and leukocyte entrance to sites of inflammation. Eur J Immunol. 2009;39(12):3477-8.

40. Laurent TC, Fraser J. Hyaluronan. The FASEB Journal. 1992;6(7):2397-404.

41. Li R, Oteiza A, Sørensen KK, McCourt P, Olsen R, Smedsrød B, et al. Role of liver sinusoidal endothelial cells and stabilins in elimination of oxidized low-density lipoproteins. American Journal of Physiology-Gastrointestinal and Liver Physiology. 2011;300(1):G71-8.

42. Park SY, Kim SY, Jung MY, Bae DJ, Kim IS. Epidermal growth factor-like domain repeat of stabilin-2 recognizes phosphatidylserine during cell corpse clearance. Mol Cell Biol. 2008;28(17):5288-9.

43. Harris EN, Weigel PH. The ligand-binding profile of HARE: Hyaluronan and chondroitin sulfates A, C, and D bind to overlapping sites distinct from the sites for heparin, acetylated low-density lipoprotein, dermatan sulfate, and CS-E. Glycobiology. 2008;18(8):638-4.

44. Harris EN, Weigel JA, Weigel PH. The human hyaluronan receptor for endocytosis (HARE/stabilin-2) is a systemic clearance receptor for heparin. J Biol Chem. 2008;283(25):17341-50.

45. Harris EN, Baggenstoss BA, Weigel PH. Rat and human HARE/stabilin-2 are clearance receptors for high-and low-molecular-weight heparins. American Journal of Physiology-Gastrointestinal and Liver Physiology. 2009;296(6):G1191-9.

46. Pempe EH, Xu Y, Gopalakrishnan S, Liu J, Harris EN. Probing structural selectivity of synthetic heparin binding to stabilin protein receptors. J Biol Chem. 2012;287(25):20774-83.

47. Zhou B, Weigel JA, Fauss LA, Weigel PH. Identification of the hyaluronan receptor for endocytosis (HARE). J Biol Chem. 2000;275(48):37733-41.

48. Deaciuc IV, Bagby GJ, Lang CH, Skrepnik N, Spitzer JJ. Gram-negative bacterial lipopolysaccharide impairs hyaluronan clearance in vivo and its uptake by the isolated, perfused rat liver. Hepatology. 2005;18(1):173-8.

49. Xu H, Lee CY, Clemens MG, Zhang JX. Pronlonged hypothermic machine perfusion preserves hepatocellular function but potentiates endothelial cell dysfunction in rat livers. Transplantation. 2004;77(11):1676-82.

50. Magnusson S, Berg T. Extremely rapid endocytosis mediated by the mannose receptor of sinusoidal endothelial rat liver cells. Biochem J. 1989;257(3):651.

51. Mousavi SA, Sporstøl M, Fladeby C, Kjeken R, Barois N, Berg T. Receptor-mediated endocytosis of immune complexes in rat liver sinusoidal endothelial cells is mediated by FcγRIIb2. Hepatology. 2007;46(3):871-84.

52. Lovdal T, Andersen E, Brech A, Berg T. Fc receptor mediated endocytosis of small soluble immunoglobulin G immune complexes in kupffer and endothelial cells from rat liver. J Cell Sci. 2000;113(18):3255-66.

53. Knolle P, Protzer U, Duchmann R, Schmitt E, ZUM B, SCHENFELDE KHM, et al. Regulation of endotoxin-induced IL-6 production in liver sinusoidal endothelial cells and kupffer cells by IL-10. Clinical & Experimental Immunology. 2003;107(3):555-61.

54. Rieder H, Ramadori G, Dienes HP, Zum Büschenfelde KHM. Sinusoidal endothelial cells from guinea pig liver synthesize and secrete cellular fibronectin in vitro. Hepatology. 1987;7(5):856-64.

55. Rieder H, Ramadori G, Meyer zum Büschenfelde K. Sinusoidal endothelial liver cells in vitro release endothelin—Augmentation by transforming growth factorβ and kupffer cell-conditioned media. Journal of Molecular Medicine. 1991;69(9):387-91.

56. Schaffner F, Poper H. Capillarization of hepatic sinusoids in man. Gastroenterology. 1963;44:239.

57. Xie G, Wang X, Wang L, Wang L, Atkinson RD, Kanel GC, et al. Role of differentiation of liver sinusoidal endothelial cells in progression and regression of hepatic fibrosis in rats. Gastroenterology. 2011.

58. Wisse E, De Zanger R, Charels K, Van Der Smissen P, McCuskey R. The liver sieve: Considerations concerning the structure and function of endothelial fenestrae, the sinusoidal wall and the space of disse. Hepatology. 2005;5(4):683-92.

59. Simon-Santamaria J, Malovic I, Warren A, Oteiza A, Le Couteur D, Smedsrød B, et al. Age-related changes in scavenger Receptor–Mediated endocytosis in rat liver sinusoidal endothelial cells. The Journals of Gerontology Series A: Biological Sciences and Medical Sciences. 2010;65(9):951.

60. Aziz-Seible RS, Casey CA. Fibronectin: Functional character and role in alcoholic liver disease. World journal of gastroenterology: WJG. 2011;17(20):2482.

61. Angulo P. Nonalcoholic fatty liver disease. N Engl J Med. 2002;346(16):1221-3.

62. Fabbrini E, Sullivan S, Klein S. Obesity and nonalcoholic fatty liver disease: Biochemical, metabolic, and clinical implications. Hepatology. 2009;51(2):679-8.

63. Nseir W, Nassar F, Assy N. Soft drinks consumption and nonalcoholic fatty liver disease. World journal of gastroenterology: WJG. 2010;16(21):2579.

64. Marchesini G, Brizi M, Bianchi G, Tomassetti S, Bugianesi E, Lenzi M, et al. Nonalcoholic fatty liver disease a feature of the metabolic syndrome. Diabetes. 2001;50(8):1844-50.

65. Utzschneider KM, Kahn SE. The role of insulin resistance in nonalcoholic fatty liver disease. Journal of Clinical Endocrinology & Metabolism. 2006;91(12):4753-61.

66. DeLeve LD, Wang X, Guo Y. Sinusoidal endothelial cells prevent rat stellate cell activation and promote reversion to quiescence. Hepatology. 2008;48(3):920-3.

67. Pasarín M, La Mura V, Gracia-Sancho J, García-Calderó H, Rodríguez-Vilarrupla A, García-Pagán JC, et al. Sinusoidal endothelial dysfunction precedes inflammation and fibrosis in a model of NAFLD. PloS one. 2012;7(4):e32785.

68. Farrell GC, Teoh N, McCuskey R. Hepatic microcirculation in fatty liver disease. The Anatomical Record: Advances in Integrative Anatomy and Evolutionary Biology. 2008;291(6):684-92.

69. Suzuki A, Angulo P, Lymp J, Li D, Satomura S, Lindor K. Hyaluronic acid, an accurate serum marker for severe hepatic fibrosis in patients with non-alcoholic fatty liver disease. Liver International. 2005;25(4):779-86.

70. Iredale JP. Models of liver fibrosis: Exploring the dynamic nature of inflammation and repair in a solid organ. J Clin Invest. 2007;117(3):539.

71. Elvevold K, Smedsrød B, Martinez I. The liver sinusoidal endothelial cell: A cell type of controversial and confusing identity. American Journal of Physiology-Gastrointestinal and Liver Physiology. 2008;294(2):G391-400.

72. Friedman SL. Hepatic stellate cells: Protean, multifunctional, and enigmatic cells of the liver. Physiol Rev. 2008;88(1):125-72.

73. Smedsrød B, Pertoft H, Gustafson S, Laurent T. Scavenger functions of the liver endothelial cell. Biochem J. 1990;266(2):313.

74. Alkhouri N, Carter–Kent C, Lopez R, Rosenberg WM, Pinzani M, Bedogni G, et al. A combination of the pediatric NAFLD fibrosis index and enhanced liver fibrosis test

identifies children with fibrosis. Clinical Gastroenterology and Hepatology. 2011;9(2):150,155. e1.

75. Huebert RC, Jagavelu K, Liebl AF, Huang BQ, Splinter PL, LaRusso NF, et al. Immortalized liver endothelial cells: A cell culture model for studies of motility and angiogenesis. Laboratory Investigation. 2010;90(12):1770-81.

76. Esser S, Wolburg K, Wolburg H, Breier G, Kurzchalia T, Risau W. Vascular endothelial growth factor induces endothelial fenestrations in vitro. J Cell Biol. 1998;140(4):947-59.

77. Krause P, Markus PM, Schwartz P, Unthan-Fechner K, Pestel S, Fandrey J, et al. Hepatocyte-supported serum-free culture of rat liver sinusoidal endothelial cells. J Hepatol. 2000;32(5):718-26.

78. Seglen PO. Preparation of isolated rat liver cells. Methods Cell Biol. 1976;13(1):29-83.

79. Blomhoff R, Berg T. Isolation and cultivation of rat liver stellate cells. Meth Enzymol. 1990;190:58-71.

80. Karaa A, Kamoun WS, Clemens MG. Oxidative stress disrupts nitric oxide synthase activation in liver endothelial cells. Free Radical Biology and Medicine. 2005;39(10):1320-31.

81. Knook D, Sleyster EC. Separation of kupffer and endothelial cells of the rat liver by centrifugal elutriation. Exp Cell Res. 1976;99(2):444-9.

82. Yannariello-Brown J, Zhou B, Ritchie D, Oka JA, Weigel PH. A novel ligand blot assay detects different hyaluronan-binding proteins in rat liver hepatocytes and sinusoidal endothelial cells. Biochem Biophys Res Commun. 1996;218(1):314-9.

83. Graupera M, March S, Engel P, Rodés J, Bosch J, García-Pagán JC. Sinusoidal endothelial COX-1-derived prostanoids modulate the hepatic vascular tone of cirrhotic rat livers. American Journal of Physiology-Gastrointestinal and Liver Physiology. 2005;288(4):G763-70.

84. Anderson N, Borlak J. Molecular mechanisms and therapeutic targets in steatosis and steatohepatitis. Pharmacol Rev. 2008;60(3):311-57.

85. Nannipieri M, Gonzales C, Baldi S, Posadas R, Williams K, Haffner SM, et al. Liver enzymes, the metabolic syndrome, and incident diabetes the mexico city diabetes study. Diabetes Care. 2005;28(7):1757-62.

86. Adams LA, Angulo P. Role of liver biopsy and serum markers of liver fibrosis in non-alcoholic fatty liver disease. Clin Liver Dis. 2007;11(1):25-3.

87. Kumar GL. Special stains and H&E. Connection. 2010:14.

88. Le TT, Yue S, Cheng JX. Shedding new light on lipid biology with coherent anti-stokes raman scattering microscopy. J Lipid Res. 2010;51(11):3091-102.

89. Goldin A, Beckman JA, Schmidt AM, Creager MA. Advanced glycation end products. Circulation. 2006;114(6):597-605.

90. Mirzaei H, Baena B, Barbas C, Regnier F. Identification of oxidized proteins in rat plasma using avidin chromatography and tandem mass spectrometry. Proteomics. 2008;8(7):1516-27.

91. Kopec KL, Burns D. Nonalcoholic fatty liver disease A review of the spectrum of disease, diagnosis, and therapy. Nutrition in Clinical Practice. 2011;26(5):565-76.

92. Kocabay G, Telci A, Tutuncu Y, Tiryaki B, Ozel S, Cevikbas U, et al. Alkaline phosphatase: Can it be considered as an indicator of liver fibrosis in non-alcoholic steatohepatitis with type 2 diabetes? Bratislavské lekárske listy. 2011;112(11):626.

93. Tanabe D, Kamimoto Y, Kai M, Hiraoka T, Tashiro S, Miyauchi Y. Effects of biliary obstruction on the endocytic activity in hepatocyte and liver sinusoidal endothelial cells in rats. European surgical research. 1996;28(3):201-1.

94. Enomoto K, Nishikawa Y, Omori Y, Tokairin T, Yoshida M, Ohi N, et al. Cell biology and pathology of liver sinusoidal endothelial cells. Medical Electron Microscopy. 2004;37(4):208-15.

95. Pasarín M, Abraldes JG, Rodríguez-Vilarrupla A, La Mura V, García-Pagán JC, Bosch J. Insulin resistance and liver microcirculation in a rat model of early NAFLD. J Hepatol. 2011;55(5):1095-102.

96. Laurent TC, Fraser J. Hyaluronan. The FASEB Journal. 1992;6(7):2397-404.

97. Le Couteur DG, Cogger VC, Markus A, Harvey PJ, Yin ZL, Ansselin AD, et al. Pseudocapillarization and associated energy limitation in the aged rat liver. Hepatology. 2003;33(3):537-43.

98. Wu Z, Xie Y, Morrison RF, Bucher N, Farmer SR. PPARgamma induces the insulin-dependent glucose transporter GLUT4 in the absence of C/EBPalpha during the conversion of 3T3 fibroblasts into adipocytes. J Clin Invest. 1998;101(1):22.

99. Schadinger SE, Bucher NLR, Schreiber BM, Farmer SR. PPARγ2 regulates lipogenesis and lipid accumulation in steatotic hepatocytes. American Journal of Physiology-Endocrinology and Metabolism. 2005;288(6):E1195-20.

100. Cobbe N, Marshall KM, Rao SG, Chang CW, Di Cara F, Duca E, et al. The conserved metalloprotease invadolysin localizes to the surface of lipid droplets. J Cell Sci. 2009;122(18):3414-23.

101. Magkos F, Lavoie JM, Kantartzis K, Gastaldelli A. Diet and exercise in the treatment of fatty liver. Journal of nutrition and metabolism. 2011;2012.

102. Hong F, Radaeva S, Pan H, Tian Z, Veech R, Gao B. Interleukin 6 alleviates hepatic steatosis and ischemia/reperfusion injury in mice with fatty liver disease. Hepatology. 2004;40(4):933-41.

103. Jarrar M, Baranova A, Collantes R, Ranard B, Stepanova M, Bennett C, et al. Adipokines and cytokines in non-alcoholic fatty liver disease. Aliment Pharmacol Ther. 2008;27(5):412-21.

104. Buqué X, Martínez MJ, Cano A, Miquilena-Colina ME, García-Monzón C, Aspichueta P, et al. A subset of dysregulated metabolic and survival genes is associated with severity of hepatic steatosis in obese zucker rats. J Lipid Res. 2010;51(3):500-13.

105. Guillén N, Navarro MA, Arnal C, Noone E, Arbonés-Mainar JM, Acín S, et al. Microarray analysis of hepatic gene expression identifies new genes involved in steatotic liver. Physiological genomics. 2009;37(3):187-98.

106. Tatsuguchi M, Furutani M, Hinagata J, Tanaka T, Furutani Y, Imamura S, et al. Oxidized LDL receptor gene (OLR1) is associated with the risk of myocardial infarction. Biochem Biophys Res Commun. 2003;303(1):247-50.

107. Merrell MD, Cherrington NJ. Drug metabolism alterations in nonalcoholic fatty liver disease. Drug Metab Rev. 2011;43(3):317-34.

108. Guerra Ruiz A, Casafont F, Crespo J, Cayón A, Mayorga M, Estebanez A, et al. Lipopolysaccharide-binding protein plasma levels and liver TNF-alpha gene expression in obese patients: Evidence for the potential role of endotoxin in the pathogenesis of non-alcoholic steatohepatitis. Obesity Surg. 2007;17(10):1374-80.

109. Rajalalitha P, Vali S. Molecular pathogenesis of oral submucous fibrosis–a collagen metabolic disorder. Journal of oral pathology & medicine. 2005;34(6):321-8.

110. Kontush A, Chapman MJ. Lipidomics as a tool for the study of lipoprotein metabolism. Curr Atheroscler Rep. 2010;12(3):194-201.

111. Sookoian S, Pirola CJ. Metabolic syndrome: From the genetics to the pathophysiology. Curr Hypertens Rep. 2011;13(2):149-57.

112. Xu C, Lin F, Qin S. Relevance between lipid metabolism-associated genes and rat liver regeneration. Hepatology Research. 2008;38(8):825-37.

113. Todorova B, Kubaszek A, Pihlajamäki J, Lindström J, Eriksson J, Valle TT, et al. The G-250A promoter polymorphism of the hepatic lipase gene predicts the conversion from impaired glucose tolerance to type 2 diabetes mellitus: The finnish diabetes prevention study. Journal of Clinical Endocrinology & Metabolism. 2004;89(5):2019-23.

114. Kotronen A, Seppänen-Laakso T, Westerbacka J, Kiviluoto T, Arola J, Ruskeepää AL, et al. Hepatic stearoyl-CoA desaturase (SCD)-1 activity and diacylglycerol but not ceramide concentrations are increased in the nonalcoholic human fatty liver. Diabetes. 2009;58(1):203-8.

115. Liu Q, Bengmark S, Qu S. Review the role of hepatic fat accumulation in pathogenesis of non-alcoholic fatty liver disease (NAFLD). . 2010.

116. Musso G, Gambino R, Cassader M. Recent insights into hepatic lipid metabolism in non-alcoholic fatty liver disease (NAFLD). Prog Lipid Res. 2009;48(1):1-26.

117. Sharma S, Barrett F, Adamson J, Todd A, Megson I, Zentler-Munro P, et al. Diabetic fatty liver disease is associated with specific changes in blood-borne markers. Diabetes Metab Res. 2012;28(4):343-8.

118. McHutchison JG, Blatt LM, De Medina M, Craig JR, Conrad A, Schiff ER, et al. Measurement of serum hyaluronic acid in patients with chronic hepatitis C and its relationship to liver histology. J Gastroenterol Hepatol. 2001;15(8):945-51.

119. Sadik N, Ahmed A, Ahmed S. The significance of serum levels of adiponectin, leptin, and hyaluronic acid in hepatocellular carcinoma of cirrhotic and noncirrhotic patients. Hum Exp Toxicol. 2012;31(4):311-2.

120. Utzschneider KM, Kahn SE. The role of insulin resistance in nonalcoholic fatty liver disease. Journal of Clinical Endocrinology & Metabolism. 2006;91(12):4753-61.

121. Grønbæk H, Thomsen KL, Rungby J, Schmitz O, Vilstrup H. Role of nonalcoholic fatty liver disease in the development of insulin resistance and diabetes. . 2008.

122. Rask-Madsen C, King GL. Mechanisms of disease: Endothelial dysfunction in insulin resistance and diabetes. Nature Clinical Practice Endocrinology & Metabolism. 2007;3(1):46-5.

123. Schalkwijk C, Stehouwer C. Vascular complications in diabetes mellitus: The role of endothelial dysfunction. Clin Sci. 2005;109:143-59.

124. Mantena SK, King AL, Andringa KK, Eccleston HB, Bailey SM. Mitochondrial dysfunction and oxidative stress in the pathogenesis of alcohol-and obesity-induced fatty liver diseases. Free Radical Biology and Medicine. 2008;44(7):1259-72.

125. Zou MH, Cohen RA, Ullrich V. Peroxynitrite and vascular endothelial dysfunction in diabetes mellitus. Endothelium. 2004;11(2):89-97.

126. Yang X, Ongusaha PP, Miles PD, Havstad JC, Zhang F, So WV, et al. Phosphoinositide signalling links O-GlcNAc transferase to insulin resistance. Nature. 2008;451(7181):964-9.

127. McCuskey RS, Ito Y, Robertson GR, McCuskey MK, Perry M, Farrell GC. Hepatic microvascular dysfunction during evolution of dietary steatohepatitis in mice. Hepatology. 2004;40(2):386-93.

128. Francque S, Laleman W, Verbeke L, Van Steenkiste C, Casteleyn C, Kwanten W, et al. Increased intrahepatic resistance in severe steatosis: Endothelial dysfunction, vasoconstrictor overproduction and altered microvascular architecture. Laboratory Investigation. 2012;92(10):1428-39.

129. DeLeve LD, Wang X, Kanel GC, Atkinson RD, McCuskey RS. Prevention of hepatic fibrosis in a murine model of metabolic syndrome with nonalcoholic steatohepatitis. The American journal of pathology. 2008;173(4):993-1001.

130. DeLeve LD, Wang X, Hu L, McCuskey MK, McCuskey RS. Rat liver sinusoidal endothelial cell phenotype is maintained by paracrine and autocrine regulation. American Journal of Physiology-Gastrointestinal and Liver Physiology. 2004;287(4):G757-63.

131. Lehmann CA. Saunders manual of clinical laboratory science. WB Saunders Company; 1998.

132. Martins PNA, Neuhaus P. Surgical anatomy of the liver, hepatic vasculature and bile ducts in the rat. Liver International. 2007;27(3):384-92.

133. Hyogo H, Yamagishi S, Iwamoto K, Arihiro K, Takeuchi M, Sato T, et al. Elevated levels of serum advanced glycation end products in patients with non-alcoholic steatohepatitis. J Gastroenterol Hepatol. 2007;22(7):1112-9.

134. Hansen B, Svistounov D, Olsen R, Nagai R, Horiuchi S, Smedsrød B. Advanced glycation end products impair the scavenger function of rat hepatic sinusoidal endothelial cells. Diabetologia. 2002;45(10):1379-88.

135. Targher G, Day CP, Bonora E. Risk of cardiovascular disease in patients with nonalcoholic fatty liver disease. N Engl J Med. 2010;363(14):1341-50.

136. Schledzewski K, Géraud C, Arnold B, Wang S, Gröne HJ, Kempf T, et al. Deficiency of liver sinusoidal scavenger receptors stabilin-1 and-2 in mice causes glomerulofibrotic nephropathy via impaired hepatic clearance of noxious blood factors. J Clin Invest. 2011;121(2):703.